# A BIM–IoT-Driven Digital Twin Framework for Uncertainty-Aware 4PL-Orchestrated Just-in-Time and Low-Carbon Material Delivery in Multi-Site Construction Projects

Behnam Karimi [a], Mohammad Mohammadpour Omran [a*], Hadi Sahebi [a]

[a] *Department of Industrial Engineering, Iran University of Science & Technology, Tehran, Iran*

* Corresponding author M. Mohammadpour Omran - omran@iust.ac.ir

**Abstract**

Construction material delivery in multi-site projects is challenged by uncertain demand and site readiness, limited logistics capacity, restricted storage space, and transportation-related emissions. This study develops an uncertainty-aware BIM–IoT-driven digital-twin framework for fourth-party logistics orchestration of just-in-time and low-carbon material delivery. The framework integrates BIM-based material and activity information with operational observations of project progress, shipment status, inventory, site readiness, and logistics-resource availability. A scenario-based multi-objective mixed-integer linear programming model is formulated within a rolling-horizon structure to minimize expected logistics cost, risk-adjusted delivery deviation, site congestion, and carbon emissions. Implemented decisions, immediate non-anticipative decisions, and future scenario-dependent recourse decisions are distinguished, while transportation uncertainty is represented by separating dispatch and arrival and incorporating conditional value at risk. For large-scale instances, an Event-Aware Rolling-Horizon NSGA-II is developed using scenario-linked encoding, Pareto warm starts, event-affected gene masks, adaptive operators, and hierarchical feasibility repair. Results from an Iranian steel-construction application and multi-size benchmarks show improved delivery, congestion, emission, hypervolume, and IGD+ performance relative to tested baseline policies and algorithms. The framework also yields quantitative decision rules for logistics capacity, site storage, data quality, consolidation, and carbon restrictions.

**Keywords:** Construction logistics; Digital twin; BIM–IoT; Fourth-party logistics; Conditional value at risk; Rolling-horizon optimization; Low-carbon delivery.

## 1. Introduction

The construction industry operates in a complex, fragmented, and resource-intensive environment in which the effective coordination of material flows is critical to project performance. Construction supply chains are commonly characterized by temporary project organizations, dispersed stakeholders, information asymmetry, and decentralized decision-making [1]. These characteristics often lead to delivery delays, excessive on-site inventories, material re-handling, space congestion, workflow interruptions, cost overruns, and reduced productivity [2]. The problem becomes more difficult in multi-site construction projects, where several sites compete simultaneously for supplier capacity, transportation resources, unloading facilities, and limited laydown areas.

Unlike repetitive manufacturing systems, construction projects are location-specific and highly dependent on changing site conditions, design requirements, installation sequences, and actual project progress. Therefore, material demand cannot be treated as a static quantity derived only from the baseline schedule. Previous studies on construction material supply channels, construction supply chain network design, project supply chains, supplier selection, and project scheduling confirm that material planning, transportation decisions, and project execution are strongly interdependent [3–7]. However, many existing planning approaches still rely on static assumptions and fragmented coordination, making them less effective when site readiness, activity progress, or logistics availability changes during project execution.

Just-in-time material delivery provides an important mechanism for reducing unnecessary inventory, improving site organization, minimizing material damage, and supporting workflow continuity. Nevertheless, its implementation in construction is challenging because construction sites often face limited storage capacity, restricted access routes, variable unloading conditions, crane availability constraints, safety requirements, and delivery time windows. A delivery plan that is efficient from a transportation perspective may still be infeasible at the site level if it creates congestion, re-handling, or interference with ongoing activities. Accordingly, construction logistics should be planned as an integrated and adaptive decision problem rather than as a set of isolated transportation tasks.

Third-party logistics providers have been increasingly used in construction to execute transportation and logistics activities [8, 9]. However, 3PL arrangements often remain tactical and execution-oriented, while multi-site construction environments require a higher level of strategic coordination [10]. Fourth-party logistics offers a suitable structure for addressing this gap. A 4PL provider can operate as a logistics control tower that integrates suppliers, 3PL providers, consolidation centers, construction sites, and information systems. Instead of merely executing deliveries, the 4PL provider can coordinate supplier selection, 3PL assignment, shipment consolidation, route selection, delivery scheduling, and adaptive replanning when operational deviations occur.

The effectiveness of such a 4PL-based logistics system depends strongly on the availability of reliable digital information. Industry 4.0 technologies, including IoT, BIM, artificial intelligence, and digital twins, provide new opportunities for real-time visibility, cyber-physical integration, and data-driven decision-making in construction and industrial systems [11–13]. BIM can provide structured information about material quantities, spatial requirements, activity dependencies, and installation sequences [14, 15], while IoT technologies can support real-time monitoring of vehicles, materials, site readiness, unloading conditions, and storage occupancy [16–18]. Recent research also emphasizes that the integration of IoT with BIM, blockchain, and digital twins can improve transparency, traceability, and coordination in construction supply chain management [19, 20].

Digital twin technology provides a dynamic virtual representation of the physical logistics system and enables periodic and event-triggered synchronization between planned and actual conditions [21]. In construction logistics, a digital twin can represent suppliers, consolidation centers, 3PL providers, transportation vehicles, construction sites, material inventories, delivery windows, and project progress. Prior studies have shown the potential of digital twins for logistics transportation management and supply chain coordination in modular construction [22, 23]. However, many digital twin applications still focus mainly on monitoring, visualization, or disruption response rather than optimization-enabled, just-in-time, and low-carbon logistics control.

Environmental performance is another essential dimension of construction supply chain decision-making. Construction logistics contributes to carbon emissions through fuel consumption, inefficient routing, repeated deliveries, low vehicle utilization, and poor shipment consolidation. Sustainable construction planning and green 4PL network design studies indicate that logistics decisions should be aligned not only with cost and time but also with environmental objectives [24, 25]. At the same time, inventory management and project scheduling studies in construction show that delivery decisions must also account for site-space limitations, resource constraints, uncertainty, and project execution requirements [26–28].

Despite these developments, the literature still lacks an integrated decision-support framework that combines 4PL coordination, BIM–IoT data integration, digital twin updating, just-in-time delivery, site-space feasibility, adaptive resequencing, and low-carbon logistics optimization in multi-site construction projects. Existing studies provide valuable insights into construction supply chain planning, digital technologies, 4PL coordination, and sustainable logistics, but these streams remain insufficiently connected for the specific problem of dynamic construction material delivery.

To address the identified gaps, this study develops an uncertainty-aware BIM–IoT-driven digital-twin framework for 4PL-orchestrated material delivery in multi-site construction projects. The digital twin functions as a logistics-control representation that synchronizes BIM-based material and activity information with operational observations of project progress, shipment status, inventory, site readiness, and logistics-resource availability. The updated state is used to construct scenario-dependent demand, priority, travel-time, capacity, route, and site-readiness parameters for a rolling-horizon optimization model.

The proposed model supports supplier assignment, logistics-provider selection, consolidation-center use, shipment dispatch, transportation routing, delivery timing, site-inventory control, and adaptive recourse. It distinguishes previously implemented decisions from immediate non-anticipative decisions and future scenario-dependent decisions. The model jointly evaluates expected logistics cost, risk-adjusted delivery deviation, site congestion, and transportation-related carbon emissions.

For large-scale implementation, the study develops an Event-Aware Rolling-Horizon NSGA-II. The algorithm retains the established non-dominated sorting and crowding-distance mechanisms of NSGA-II but introduces a scenario-linked chromosome, rolling-horizon Pareto warm start, event-affected gene mask, site–material block crossover, priority- and risk-guided adaptive mutation, and hierarchical scenario-feasibility repair.

Accordingly, the study addresses the following research questions:

RQ1. How can BIM-based project information and IoT-based operational observations be integrated into an operational digital twin for 4PL-controlled construction material delivery?

RQ2. How can demand, transportation time, supplier and logistics capacity, route availability, and site readiness be incorporated into an uncertainty-aware rolling-horizon material-delivery model?

RQ3. To what extent does the proposed ERH-NSGA-II improve Pareto convergence, objective-space coverage, feasibility, and event-response performance relative to established multi-objective solution methods?

RQ4. Which operational thresholds and parameter interactions should guide 4PL decisions regarding transportation reserve, site storage, IoT-data quality, consolidation capacity, and carbon restrictions?

The methodological contribution of this study does not lie merely in combining BIM, IoT, digital twin technology, and 4PL coordination. Rather, the study makes four interrelated contributions. First, the study develops an operational digital-twin architecture for construction logistics that connects physical material flows, data acquisition and validation, digital-state synchronization, uncertainty representation, optimization, execution, and feedback. Unlike monitoring-oriented digital-twin applications, the proposed architecture explicitly maps updated operational states into optimization parameters and executable 4PL decisions. Second, an uncertainty-aware multi-objective rolling-horizon model is formulated for 4PL-orchestrated construction material delivery. The model distinguishes implemented decisions, immediate non-anticipative decisions, and future scenario-dependent recourse decisions. It also separates shipment dispatch from material arrival and incorporates delivery-risk CVaR alongside cost, congestion, and carbon objectives. Third, the study develops ERH-NSGA-II as a problem-specific solution method. Its contribution does not lie in standard non-dominated sorting or crowding-distance selection, but in its two-stage scenario-linked chromosome, rolling-horizon Pareto warm start, event-affected gene mask, block crossover, adaptive mutation, and hierarchical feasibility-repair mechanisms. Fourth, the framework is evaluated using an Iranian multi-site construction case application and reproducible benchmark instances evaluated with 30 independent seeds per algorithm–instance combination. Exact verification, comparisons with NSGA-II, MOEA/D, and NSGA-III, statistical tests, scalability assessment, and component-level ablation are used to evaluate algorithmic behavior. The sensitivity and interaction analyses additionally translate the results into quantitative operational decision rules.

It should be noted that the study does not claim that digital twins, NSGA-II, CVaR, or rolling-horizon optimization are individually new concepts. Its methodological contribution lies in their construction-specific integration and in the development of problem-specific modeling and search mechanisms for uncertainty-aware, multi-site, 4PL-controlled material delivery. Accordingly, the proposed framework is positioned as a closed-loop prescriptive control approach rather than as a simple integration of existing digital technologies. Its distinguishing feature is the explicit linkage between physical-system observations, digital-twin state estimation, optimization-parameter updating, uncertainty-aware decision production, and feedback to the physical logistics network. This closed-loop linkage differentiates the proposed approach from BIM-enabled logistics models that use static project information, monitoring-oriented digital twins that do not produce prescriptive delivery decisions, and conventional 4PL models that do not account for construction-specific site and project-progress conditions.

The remainder of the paper is organized as follows. Section 2 reviews the relevant literature and positions the study within construction logistics, 4PL coordination, BIM–IoT integration, digital twins, uncertainty-aware optimization, and low-carbon delivery planning. Section 3 presents the problem description, operational digital-twin architecture, state-updating mechanism, and uncertainty representation. Section 4 develops the uncertainty-aware multi-objective rolling-horizon mathematical model. Section 5 presents the digital-twin updating procedure and ERH-NSGA-II solution method. Section 6 describes the case application, uncertainty scenarios, benchmark instances, comparison algorithms, and experimental protocol. Section 7 reports the case results, exact verification, comparative and statistical results, scalability, sensitivity and interaction analyses, event-response ablation, and quantitative managerial decision rules. Section 8 concludes the study and discusses its limitations and future research directions.

## 2. Literature Review

This section reviews the literature streams relevant to BIM–IoT-driven digital twin-based 4PL coordination for just-in-time and low-carbon material delivery in multi-site construction projects. The review is organized into five areas: construction supply chain and material logistics planning, 4PL coordination, BIM–IoT-enabled digital transformation, digital twin-enabled logistics control, and low-carbon just-in-time construction logistics. The final subsection summarizes the research gap addressed in this study.

### 2.1. Construction supply chain and material logistics planning

Construction supply chain management has received considerable attention because material availability, delivery reliability, supplier coordination, and logistics planning directly affect project cost, schedule performance, site productivity, and environmental outcomes. Construction supply chains are project-based, temporary, and strongly influenced by site-specific conditions. As a result, material planning becomes particularly complex in multi-site environments where projects compete for limited supplier capacity, transportation resources, and storage space.

Early optimization-oriented studies contributed to formalizing construction material planning as a quantitative decision problem. Jaśkowski et al. developed a decision model for planning material supply channels in construction, emphasizing the need to select supply alternatives according to project and logistics requirements [3]. Golpîra integrated facility location, supplier selection, and inventory decisions into a multi-project construction supply chain network design model under vendor-managed inventory [4]. Abdzadeh et al. proposed a project supply chain model focusing on material flow and transportation quality, while Asadujjaman et al. integrated multi-project scheduling, material ordering, and supplier selection [5, 6]. Chen et al. further incorporated environmental and resilience considerations into construction material sourcing under uncertainty [7]. These studies show that construction logistics decisions should not be optimized separately from project execution.

Recent construction supply chain studies have also highlighted the importance of inventory management, project scheduling, and site-level operational constraints. Putra et al. showed that improving inventory management can enhance supply chain management performance in residential construction [26]. Imannezhad and Avakh Darestani addressed resource-constrained project scheduling with activity interruption in construction projects, while Salmasnia et al. incorporated time, cost, and environmental objectives under uncertainty [27, 28]. These studies are relevant because material delivery plans must account not only for transportation efficiency but also for project timing, resource availability, uncertainty, and environmental impact.

Site-space feasibility is another critical issue. Mei et al. proposed an integrated optimization and visualization approach for construction site layout planning considering primary and reuse building materials [29]. Their findings reinforce the idea that material delivery decisions should be coordinated with laydown areas, access routes, unloading capacity, and site congestion. A delivery plan that ignores site-space limitations may reduce transportation cost but increase re-handling, safety risks, blocked access, and productivity losses.

### 2.2. Fourth-party logistics coordination in supply chain management

Fourth-party logistics has emerged as a strategic approach for coordinating complex logistics networks. Unlike 3PL providers, which mainly execute transportation, warehousing, or distribution activities, a 4PL provider acts as an integrator that coordinates logistics service providers, information flows, resources, and decision processes. This distinction is important in construction projects because delivery decisions must be synchronized with project progress, supplier capacity, site readiness, unloading limitations, and installation requirements.

Büyüközkan et al. evaluated 4PL operating models using a Choquet integral-based decision-making approach and highlighted 4PL as a strategic logistics management structure rather than a simple outsourcing arrangement [30]. Huang et al. formulated a fourth-party logistics routing problem with fuzzy duration time, showing that uncertainty in execution time should be incorporated into 4PL routing decisions [31]. Yin et al. developed a 4PL network design model under uncertain conditions, while Zhang et al. proposed a green 4PL network design model under a carbon cap-and-trade policy [25, 32]. These studies provide important foundations for logistics orchestration, routing, provider selection, uncertainty handling, and green logistics.

However, most 4PL studies are developed for general logistics or supply chain networks and do not fully address construction-specific requirements. Construction material delivery involves limited laydown areas, unloading capacities, installation-related delivery windows, site accessibility constraints, and project progress-dependent demand. Moreover, conventional 4PL models rarely integrate BIM-based material requirements, IoT-based site monitoring, or digital twin-based adaptive replanning. Therefore, there is a need to adapt the 4PL concept into a construction-specific control tower that can coordinate logistics decisions dynamically.

### 2.3. BIM–IoT-enabled digital transformation in construction supply chains

Digital technologies have become important enablers of construction supply chain integration. BIM provides structured project information, including material quantities, spatial relationships, activity dependencies, installation sequences, and design-related constraints. Ghannadpour et al. showed that BIM influences several construction project management knowledge areas and can support more integrated project planning and control [15]. Metvaei et al. demonstrated how BIM-enabled robotic manufacturing can link design information to downstream production decisions in prefabricated buildings [14]. Rangasamy and Yang further emphasized the convergence of BIM, AI, and IoT as a key direction for connected prefabricated construction systems [16].

IoT technologies complement BIM by enabling real-time data capture from the physical logistics environment. Zhang et al. developed a cost evaluation model for IoT-enabled prefabricated construction supply chain management, highlighting the operational and economic value of digital visibility [13]. Ben-Daya et al. reviewed IoT applications in supply chain management and emphasized visibility, traceability, monitoring, and information sharing as key benefits [33]. Pittri et al. provided a systematic review of IoT in construction supply chain management and showed that IoT applications have evolved from isolated tracking solutions toward integrated ecosystems involving BIM, blockchain, and digital twins [19]. Hasheminasab et al. reviewed the challenges and drivers of IoT adoption in supply chains, while Islahudin et al. showed how IoT-enabled monitoring can support real-time scheduling and agile operational decisions [17, 18].

Industry 4.0 studies also support this direction. Nazzal emphasized that digital transformation in construction requires not only technology adoption but also leadership, organizational alignment, and managerial readiness [12]. Lahmine and Bennouna reviewed the contribution of AI, blockchain, IoT, and big data to quality management, while Bahtat et al. discussed the role of IoT, digital twins, and artificial intelligence in reconfigurable Industry 4.0 systems [11, 34]. These studies suggest that the success of digital construction logistics depends on both technological integration and coordinated decision-making.

### 2.4. Digital twin-enabled logistics control

Digital twin technology provides a dynamic virtual representation of a physical system that is continuously updated through data exchange with its real-world counterpart [21]. In construction logistics, a digital twin can represent suppliers, 3PL providers, consolidation centers, vehicles, construction sites, material inventories, site capacities, delivery windows, and project progress. This capability makes digital twins suitable for monitoring, prediction, simulation, and optimization of logistics decisions.

Li and Wang investigated digital twin-driven management strategies for logistics transportation systems and emphasized the potential of digital twins for real-time monitoring and dynamic optimization [22]. Lee and Lee developed a digital twin for supply chain coordination in modular construction and used it to evaluate coordination policies [23]. Yu and Shenle proposed a federated digital twin's platform for smart city logistics, highlighting the value of collaborative data sharing among multiple actors [35]. Le and Fan reviewed digital twins for logistics and supply chain systems and identified visibility, scenario evaluation, data integration, and decision automation as central capabilities [36].

The integration of BIM, IoT, and blockchain has also been explored in modular construction supply chain management. Li et al. proposed a blockchain-enabled IoT–BIM platform for modular construction, showing how integrated digital platforms can improve transparency, traceability, and data-information-knowledge management across fragmented supply chains [20]. Such studies show that digital twins and complementary technologies can support more reliable and coordinated construction logistics. However, many existing applications still emphasize monitoring, visualization, or traceability rather than optimization-enabled just-in-time delivery control. This study therefore positions the digital twin as a prescriptive decision environment that supports adaptive delivery planning under site, logistics, and environmental constraints.

### 2.5. Low-carbon and just-in-time construction logistics

Low-carbon logistics has become increasingly important as construction projects face growing pressure to reduce environmental impacts. Material transportation generates emissions through vehicle movements, fuel consumption, inefficient routing, repeated deliveries, low vehicle utilization, and poor shipment consolidation. Sustainable construction planning therefore requires the integration of project management, supply chain coordination, and environmental objectives [24]. Green 4PL research also shows that carbon policies can be embedded directly into logistics network design and provider coordination decisions [25].

Just-in-time delivery and low-carbon delivery may reinforce or conflict with each other. Shipment consolidation can reduce vehicle movements and emissions, but it may reduce delivery flexibility. Delivering materials exactly when needed can reduce site inventory and congestion, but it may require more frequent trips. Selecting low-emission routes or logistics providers can improve environmental performance, but it may influence delivery time and site readiness. These trade-offs justify the use of multi-objective optimization models that simultaneously consider logistics cost, delivery timing, site congestion, and transportation-related carbon emissions.

### 2.6. Research gaps and positioning of the present study

The reviewed literature shows substantial progress in construction supply-chain planning, 4PL coordination, BIM–IoT integration, digital twins, uncertainty-aware optimization, and low-carbon logistics [3–7, 13, 17–36]. However, relatively few studies integrate these elements within a single framework for multi-site construction material delivery. Existing models often address sourcing, transportation, inventory, scheduling, or site layout separately, while 4PL studies rarely incorporate construction-specific constraints such as limited storage, unloading capacity, site readiness, and progress-dependent demand. Similarly, many digital-twin applications emphasize monitoring, visibility, or disruption detection rather than closed-loop optimization and adaptive logistics control.

To address this gap, this study develops an uncertainty-aware BIM–IoT-driven digital-twin framework for 4PL-orchestrated just-in-time and low-carbon material delivery. The framework links validated operational observations to state updating, scenario construction, rolling-horizon optimization, execution, and feedback. It jointly considers supplier and 3PL selection, consolidation, routing, dispatch and arrival timing, site capacity, delivery risk, and carbon emissions. The contribution therefore lies not in introducing these concepts individually, but in their construction-specific integration and in the development of the ERH-NSGA-II solution method for adaptive multi-site logistics planning.

## 3. Problem Description

This study addresses the problem of just-in-time and low-carbon material delivery in multi-site construction projects under the coordination of a fourth-party logistics provider. The considered system consists of material suppliers, consolidation centers, 3PL providers, transportation vehicles, and multiple construction sites. Each construction site has project-specific material requirements, installation priorities, unloading limitations, delivery time windows, access conditions, and limited temporary storage capacity. At the same time, suppliers and 3PL providers operate under limited capacities, heterogeneous cost structures, different service characteristics, and varying emission performance. These characteristics make material delivery planning a complex coordination problem in which project demand, logistics capacity, site readiness, delivery timing, and environmental performance must be considered simultaneously. The problem is developed under the assumptions that material-quality requirements are satisfied, construction sites have predefined receiving time windows and storage limits, and BIM–IoT data are sufficiently reliable to update demand, site readiness, shipment status, and logistics availability. At each update epoch, the current validated state of the system is assumed to be known, whereas future demand, travel times, supplier availability, logistics capacity, site readiness, and selected operational observations may vary across scenarios. Material-quality requirements and the structural configuration of the logistics network are assumed to remain fixed and known throughout each planning run.

The 4PL provider acts as the central logistics orchestrator of the network. It does not necessarily own physical transportation assets, but coordinates suppliers, 3PL providers, consolidation centers, and construction sites through a digital control tower. Materials can be transported directly from suppliers to construction sites or indirectly through consolidation centers, where shipments may be combined, temporarily stored, sorted, and dispatched according to site-specific delivery priorities. The 4PL provider is responsible for determining supplier assignments, 3PL assignments, delivery quantities, shipment timing, route selection, consolidation center usage, and adaptive changes in delivery plans when operational conditions change. The overall structure of the proposed framework is illustrated in Figure 1.

The proposed framework integrates BIM-based planning data and IoT-based operational data within a digital twin environment. BIM provides structured information on material quantities, activity relationships, installation sequences, spatial requirements, and planned delivery windows. IoT technologies provide real-time or near-real-time data on vehicle locations, shipment status, site progress, unloading availability, material arrival, and storage occupancy. The digital twin combines these data streams to maintain an updated virtual representation of the construction logistics system. This environment supports real-time visibility, demand updating, conflict detection, parameter revision, and optimization-based decision-making.

### 3.1. Digital-twin-based parameter updating mechanism

The digital twin does not transfer raw IoT observations directly into the optimization model. Instead, it contains a data-processing and state-estimation layer that combines BIM-based planning information with validated observations from the physical logistics system. This layer converts the updated physical-system state into time-indexed model parameters before each optimization run. Accordingly, the material-demand parameter and the delivery-priority parameter are calculated parameters rather than direct sensor measurements.

- **Updated material-demand parameter**

The parameter $D_{\mathrm{pmt}}$ represents the quantity of material $m$ expected to be consumed at construction site $p$ during planning period $t$. Its baseline value is derived from the BIM-based material quantities and the planned execution sequence of the associated construction activities. During project execution, the timing of material consumption is revised according to the updated progress state of those activities. Therefore, BIM determines the quantity and activity–material relationship, while operational observations update the time period in which the material is expected to be required.

$$D_{pmt}^{(k)} = \sum_{a \in A_{pm}} Q_{pma} \left[\hat{\rho}_{pa,t}^{(k)} - \hat{\rho}_{pa,t-1}^{(k)}\right]^{+} \tag{1}$$

where $A_{pm}$ is the set of activities at site $p$ that consume material m; $Q_{pma}$ is the BIM-based material quantity assigned to activity $a$; $k$ denotes the digital-twin update epoch; and $\hat{\rho}_{pa,t}^{(k)}$ is the updated forecast of the cumulative completion ratio of activity a by the end of period $t$. The positive-part operator prevents a negative period demand when the activity forecast is revised.

Equation (1) is applied in the digital-twin preprocessing layer. At each update epoch, the resulting values of $D_{pmt}^{(k)}$ are passed to the model as known input parameters.

- **Updated delivery-priority parameter**

The parameter $Pr_{\text{pmt}}$ is a dimensionless weight representing the relative urgency of making material $m$ available at site $p$ during period $t$. It is calculated by the digital-twin processing layer from the current project and logistics state. The priority value increases when the associated construction activity is more critical, when the projected material shortage is larger, or when the expected material-arrival time is more likely to exceed the required availability time.

$$
\begin{gathered}
Pr_{pmt}^{(k)} = 1 + (Pr^{\max} - 1)\Psi_{pmt}^{(k)} \\
\Psi_{pmt}^{(k)} = \lambda_C C_{pmt}^{(k)} + \lambda_S S_{pmt}^{(k)} + \lambda_L L_{pmt}^{(k)} \\
\lambda_C + \lambda_S + \lambda_L = 1 \\
0 \le C_{pmt}^{(k)}, S_{pmt}^{(k)}, L_{pmt}^{(k)} \le 1 \\
1 \le Pr_{pmt}^{(k)} \le Pr^{max}
\end{gathered} \tag{2}
$$

In Eq. (2), $C_{pmt}^{(k)}$, $S_{pmt}^{(k)}$, and $L_{pmt}^{(k)}$ respectively denote the normalized activity-criticality, projected-shortage, and predicted-lateness components. The coefficients $\lambda_C$, $\lambda_S$, and $\lambda_L$ are non-negative policy parameters that express the relative importance of the three components. $Pr^{max}$ defines the maximum allowable priority weight. The implemented priority scale and component weights, together with their selection rule, are reported in Table 7. Here, Ψ denotes the composite normalized urgency score defined by the weighted sum in Eq. (2).

$$
C_{pmt}^{(k)} = \max_{a \in A_{pm}} \left[ 1 - min\left(1, \frac{TF_{pa}^{(k)}}{TF^{max}}\right) \right] \tag{3}
$$

The activity-criticality component in Eq. (3) is obtained from the updated project schedule. $TF_{pa}^{(k)}$ represents the total float of activity a, and $TF^{max}$ is a normalization parameter. Materials associated with critical or near-critical activities receive larger criticality values.

$$
\begin{gathered}
S_{pmt}^{(k)} = \min\left(1, \sigma_{pmt}^{(k)}\right) \\
\sigma_{pmt}^{(k)} = \frac{\max\left(0, D_{pmt}^{(k)} - AI_{pmt}^{(k)}\right)}{\max\left(D_{pmt}^{(k)}, \varepsilon\right)}
\end{gathered} \tag{4}
$$

The projected-shortage component in Eq. (4) compares the updated demand with the material quantity expected to be available at the site. $AI_{pmt}^{(k)}$ includes the validated site inventory and confirmed inbound material expected to be available before the required time. In Eq. (4), σ denotes the normalized shortfall ratio; the numerator uses the non-negative demand shortfall, and ε is a small positive constant that prevents division by zero when updated period demand is zero.

$$
\begin{gathered}
L_{pmt}^{(k)} = \min\left(1, \ell_{pmt}^{(k)}\right) \\
\ell_{pmt}^{(k)} = \frac{\max\left(0, \widehat{AT}_{pmt}^{(k)} - T_{pmt}^{req}\right)}{Delay^{\max}}
\end{gathered} \tag{5}
$$

The predicted-lateness component in Eq. (5) compares the estimated material-arrival time $\widehat{AT}_{pmt}^{(k)}$ with the required material-availability time $T_{pmt}^{req}$. $Delay^{max}$ is a normalization parameter representing the maximum delay considered in the priority calculation. In Eq. (5), ℓ denotes the normalized non-negative lateness ratio; both ℓ and the final lateness component are capped at one.

The operational observations used in the updating process may include project-progress status, site inventory, shipment status, estimated arrival time, site readiness, unloading availability, and logistics-resource availability. The specific data-acquisition technologies depend on the implementation environment and are therefore not fixed in the general framework. Regardless of the technology used, observations must be timestamped, validated, and mapped to the corresponding construction site, material, activity, shipment, or logistics resource before they are used for parameter updating.

The delivery-priority parameter affects the penalty associated with early or late material availability and does not override the physical feasibility constraints. A highly prioritized material cannot be delivered when the construction site is unavailable, when unloading capacity is insufficient, or when the site-storage constraint would be violated. Site availability, unloading capacity, and storage capacity therefore remain separate model parameters and constraints.

### 3.2. Operational architecture of the digital twin

The proposed digital twin is structured as a closed-loop decision-support architecture that connects the physical construction logistics system with its digital representation and optimization model. The architecture is technology-neutral and does not depend on a specific sensing device, communication protocol, software platform, or database technology. Instead, it specifies the functional components and information exchanges required to acquire operational observations, estimate the current logistics state, update the model parameters, produce revised delivery decisions, and communicate those decisions to the physical system. The present study develops and computationally evaluates an operational decision architecture for a digital-twin-enabled logistics control system; it does not report a fully deployed industrial cyber-physical implementation.

The operational architecture consists of six functional layers: (1) the physical logistics layer, (2) the data-acquisition layer, (3) the data-integration and validation layer, (4) the digital-state layer, (5) the decision and optimization layer, and (6) the execution and feedback layer.

1) **Physical logistics layer:** The physical logistics layer represents the real construction supply network, including material suppliers, logistics providers, transportation resources, consolidation centers, construction sites, material inventories, receiving facilities, and unloading resources. Changes in this layer, such as project-progress deviations, shipment delays, resource unavailability, or site-capacity changes, produce the operational events that may require an update of the digital representation and delivery plan.
2) **Data-acquisition layer:** The data-acquisition layer collects observations describing the current condition of the physical logistics system. These observations may relate to activity progress, material inventory, shipment status, estimated arrival time, site readiness, unloading availability, transportation-resource availability, supplier capacity, and consolidation-center capacity. The framework does not prescribe a specific acquisition technology; the observations may be obtained through

automated sensing, enterprise information systems, digital project records, or validated operational reporting.

3) **Data-integration and validation layer:** The data-integration and validation layer converts heterogeneous observations into consistent and usable digital-twin inputs. Each observation is associated with an entity identifier, a time stamp, a measurement unit, a data source, and a data-quality status. Before an observation is accepted, the layer performs format checking, range validation, duplicate detection, temporal consistency checking, and cross-source consistency checking. Invalid, incomplete, or outdated observations are flagged and are not directly transferred to the parameter-updating process.
If a required observation is unavailable or fails the validation rules, the digital twin applies a predefined fallback procedure. Depending on data availability, the fallback value may be obtained from the most recent validated state, an updated planning forecast, or a conservative operational estimate. The affected state variable is simultaneously assigned a reduced confidence level so that data-quality uncertainty can be considered in the subsequent decision process.

4) **Digital-state layer:** The digital-state layer maintains the most recent validated representation of the construction logistics system. It stores the status of material requirements, project progress, site readiness, inventories, shipments, transportation resources, supplier availability, logistics capacity, delivery windows, and receiving conditions. The digital state is versioned by update epoch so that each optimization result can be traced to the information available when the decision was produced.

$$X^{(k)} = \{Progress^{(k)}, Inventory^{(k)}, ShipmentStatus^{(k)}, SiteStatus^{(k)}, ResourceStatus^{(k)}\} \quad (6)$$

In Eq. (6), $X^{(k)}$ denotes the validated digital-twin state at update epoch $k$. The state includes project-progress, inventory, shipment, site, resource, capacity, and data-quality information. The exact dimensionality of the state depends on the number of sites, materials, logistics resources, and planning periods considered in a particular application.

5) **Decision and optimization layer:** The decision and optimization layer transforms the validated digital state into updated model parameters and delivery decisions. The parameter-updating mechanism described in Section 3.1 calculates D_{pmt}, Pr_{pmt}, site availability, storage occupancy, unloading capacity, supplier capacity, logistics-provider capacity, and other time-dependent model inputs. The revised parameter set is then transferred to the multi-objective optimization model.

$$\Theta^{(k)} = G\left(X^{(k)}, B\right) \quad (7)$$

In Eq. (7), $\Theta^{(k)}$ is the set of model parameters used at update epoch $k$, $B$ represents the baseline BIM and project-planning information, and $G(.)$ denotes the parameter-transformation mechanism. The parameter set includes both relatively stable network parameters and dynamically updated operational parameters.

$$U^{(k)} = O\left(\Theta^{(k)}, U^{implemented}\right) \quad (8)$$

In Eq. (8), $U^{(k)}$ represents the revised logistics decisions produced at update epoch $k$, $U^{implemented}$ represents decisions that have already been executed and cannot be changed, and $O(.)$ represents the multi-objective optimization and solution-selection procedure.

6) **Execution and feedback layer:** The execution and feedback layer communicates the selected logistics decisions to the relevant physical-system actors. The outputs may include supplier assignments, logistics-provider assignments, shipment quantities, delivery periods, route selections, consolidation decisions, and updated delivery priorities. Once the immediate decisions are implemented, their execution status is observed and returned to the data-acquisition layer. This feedback closes the loop between the physical system, the digital state, and the optimization model.

Therefore, the decision-making process consists of data acquisition, digital twin updating, optimization, implementation, and monitoring. When deviations occur in project progress, site readiness, vehicle availability, supplier capacity, or unloading conditions, the digital twin updates the relevant parameters and enables the 4PL provider to revise the delivery plan. This adaptive delivery resequencing mechanism allows delivery priorities, shipment timing, route choices, consolidation decisions, and logistics provider assignments to be adjusted according to actual conditions. As a result, the proposed framework prevents unnecessary early deliveries, reduces late deliveries, limits site congestion, and improves the synchronization between material flow and construction progress.


Figure 1. Closed-loop operational architecture of the proposed digital-twin-based 4PL framework.

The objective of the proposed problem is to develop a decision-support framework that enables the 4PL provider to plan and control construction material deliveries while balancing operational, temporal, spatial, and environmental criteria. The framework seeks to minimize logistics cost, delivery earliness and tardiness, site congestion, and transportation-related carbon emissions. Accordingly, the problem is formulated as a multi-objective logistics planning problem in which supplier selection, 3PL assignment, shipment quantities, delivery scheduling, route selection, consolidation decisions, site capacity limitations, adaptive resequencing, and carbon performance are jointly considered. Table 1 summarizes the functional components of the proposed digital-twin architecture.

Table 1. Functional components of the proposed digital-twin architecture

| Layer | Main function | Principal inputs | Principal outputs |
|---|---|---|---|

| | | | |
|---|---|---|---|
| Physical logistics | Execution of material flows and construction-logistics activities | Delivery and project decisions | Operational events and physical status |
| Data acquisition | Capture of current project and logistics observations | Physical-system status | Time-stamped observations |
| Integration and validation | Harmonization and quality control | Raw observations | Validated observations and quality flags |
| Digital state | Representation of the latest logistics condition | Validated observations and BIM baseline | Updated state $X^{(k)}$ |
| Decision and optimization | Parameter updating and logistics optimization | $X^{(k)}$, BIM baseline and implemented decisions | Updated parameters and decisions $U^{(k)}$ |
| Execution and feedback | Communication and implementation of decisions | Selected logistics plan | Execution status and new observations |

### 3.3. State synchronization and update logic

Synchronization refers to the process through which the digital representation is updated to reflect the most recent validated condition of the physical logistics system. The proposed framework uses a hybrid synchronization mechanism combining scheduled updates and event-triggered updates. Scheduled updates maintain regular consistency between planning and execution, while event-triggered updates enable an earlier response when a significant operational deviation occurs.

$$X^{(k)} = F\left(X^{(k-1)}, Y^{(k)}, B\right) \tag{9}$$

In Eq. (9), $Y^{(k)}$ denotes the set of validated observations received since the previous update epoch, $B$ denotes the baseline BIM and planning information, and $F(.)$ represents the synchronization and state-estimation process. The resulting state $X^{(k)}$ replaces the previous state only after the relevant validation and consistency rules have been satisfied.

An event-triggered update is activated when one or more monitored deviations exceed their corresponding acceptance thresholds. The framework distinguishes among project-progress, shipment, site-readiness, logistics-capacity, inventory, and data-quality events.

$$Trigger^{(k)} = \begin{cases} 1, & \max_{j \in J} \left\{ \dfrac{\left|\Delta_j^{(k)}\right|}{\tau_j} \right\} > 1 \\ 0, & otherwise \end{cases} \tag{10}$$

In Eq. (10), $J$ is the set of monitored deviation categories, $\Delta_j^{(k)}$ is the observed deviation for category $j$, and $\tau_j$ is its predefined acceptance threshold. A value of $Trigger^{(k)}$=1 initiates state synchronization, parameter updating, and replanning for the remaining planning horizon. Table 2 summarizes the operational-event categories and their parameter effects.

Table 2. Operational-event categories and their effects on digital-twin parameters

| Event category | General deviation | Potential parameter effect |
|---|---|---|
| Project progress | Actual or forecast progress differs from baseline | $D_{pmt}$ , $Pr_{pmt}$ , required delivery period |
| Shipment | Arrival or shipment status deviates from plan | ETA ،lateness risk ، available inbound inventory |
| Site readiness | Site cannot receive material as planned | $Open_{pt}$,unloading capacity |
| Logistics capacity | Supplier or logistics capacity changes | Supplier and 3PL capacity |
| Inventory | Physical inventory differs from digital record | Site or consolidation inventory |
| Data quality | Observation is missing, stale or inconsistent | Confidence level and fallback value |

The proposed digital twin supports material-delivery planning and logistics control and does not perform detailed construction-activity rescheduling. Project-progress and schedule information are treated as external planning inputs that influence material demand, delivery priority, site readiness, and required delivery timing. When a major project-schedule revision is required, the revised schedule is produced by the project-planning system and subsequently transferred to the digital twin as updated baseline information.

### 3.4. Representation of dynamic uncertainty

Although the digital twin updates the model parameters using the most recent validated observations, the future state of the construction logistics system remains uncertain. Parameter updating and uncertainty modeling therefore perform two different functions. Parameter updating estimates the current system state, whereas uncertainty modeling represents the range of conditions that may occur during the remaining planning horizon.

The proposed framework represents future uncertainty through a finite set of scenarios. Each scenario describes one possible evolution of material requirements, project progress, transportation time, supplier availability, logistics-provider capacity, route accessibility, site readiness, and data reliability. The scenarios are reconstructed or revised at each digital-twin update epoch so that the uncertainty representation remains consistent with the latest available state.

$$\Omega^{(k)} = \left\{\omega_1, \omega_2, \ldots, \omega_{|\Omega^k|}\right\} \tag{11}$$

$$\sum_{\omega \in \Omega^{(k)}} \pi_\omega^{(k)} = 1, \qquad \pi_\omega^{(k)} \geq 0 \tag{12}$$

In Eqs. (11) and (12), $\Omega^{(k)}$ is the set of uncertainty scenarios defined at digital-twin update epoch k, and $\pi_\omega^{(k)}$ is the occurrence weight or probability assigned to scenario ω. The scenario set and its associated weights may change when new observations become available.

For a general uncertain parameter θ, its value under scenario ω and period t is represented as:

$$\theta_t^\omega = \bar{\theta}_t + \Delta\theta_t^\omega \tag{13}$$

In Eq. (13), $\bar{\theta}_t$ is the current forecast or nominal parameter value derived from the digital-twin state, and $\Delta\theta_t^\omega$ represents the scenario-specific deviation from that value.

The main uncertain parameters include material demand, delivery priority, supplier capacity, logistics-provider capacity, transportation time, route availability, site availability, unloading capacity, and the initial physical-state estimates affected by imperfect operational observations. Table 3 summarizes the general sources and model representations of dynamic uncertainty.

Table 3. Sources and model representations of dynamic uncertainty

| Uncertainty source | General representation | Main affected parameters |
|---|---|---|
| Project-progress variation | Alternative progress and demand trajectories | $D_{pmt}^{\omega}$ ‘$pr_{pmt}^{\omega}$ |
| Travel-time variability | Scenario-dependent transport lag | $\ell_{spvr\tau}^{SP,\omega}$ |
| Supplier disruption | Scenario-dependent available supply | $Cap_{smt}^{S,\omega}$ |
| Logistics-resource disruption | Scenario-dependent 3PL capacity | $Cap_{vt}^{V,\omega}$ |
| Weather or route condition | Route closure or increased travel time | $RouteOpen_{ijvr\tau}^{\omega}$ ‘ $\ell_{spvr\tau}^{SP,\omega}$ |
| Site-readiness variation | Alternative receiving and unloading states | $Open_{pt}^{\omega}$ ‘$UCap_{pt}^{\omega}$ |
| Imperfect operational observations | Alternative plausible current-state values | Initial inventory, site status, shipment status |
| Demand-estimation error | Alternative material-demand values | $D_{pmt}^{\omega}$ |

The uncertainty scenarios are embedded within a rolling-horizon control process. At update epoch k, the decisions that have already been implemented are fixed. Decisions for the immediate execution period are selected before the future scenario is known and must therefore be identical across all scenarios. Decisions for later periods may differ among scenarios and represent recourse actions that can be implemented after additional information becomes available.

$$U^{implemented} \cup U_{t_0} \cup \{U_t^{\omega}: t > t_0, \omega \in \Omega^{(k)}\} \tag{14}$$

In Eq. (14), $U^{implemented}$ denotes fixed past decisions, $U_{t_0}$ denotes the common immediate decision, and $U_t^{\omega}$ denotes scenario-dependent recourse decisions for later periods.

The main manuscript presents a compact formulation; complete notation, objective expansions, and the full constraint set are provided in Supplementary Section S1.

## 4. Uncertainty-Aware Mathematical Model

This section presents an uncertainty-aware multi-objective mixed-integer linear programming formulation for the BIM–IoT-driven digital-twin framework for 4PL-orchestrated just-in-time and low-carbon material delivery in multi-site construction projects. The formulation preserves the original logistics-network structure, including suppliers, consolidation centers, 3PL providers, transportation routes, and construction sites, while explicitly representing future uncertainty through a finite set of scenarios. The model is designed for use within a rolling-horizon decision process in which previously implemented or irrevocably committed decisions are fixed, immediate decisions are made before the future scenario becomes known, and later decisions may adapt after additional information is received.

### 4.1. Model description

The model considers a multi-site construction logistics network in which different material types are supplied by multiple suppliers and transported either directly to construction sites or indirectly through consolidation centers. Transportation activities are assigned to 3PL providers and feasible routes, while the 4PL provider coordinates supplier assignment, 3PL assignment, shipment quantities, transportation routes, consolidation-center use, and delivery timing. To represent uncertain transportation time correctly, the formulation distinguishes the period in which a shipment is dispatched from the period in which it physically arrives at a consolidation center or construction site.

Four performance dimensions are considered: total logistics cost, delivery earliness and tardiness, site congestion, and transportation-related carbon emissions. Logistics cost, congestion, and emissions are evaluated through their scenario-weighted expected values. Delivery deviation is evaluated through both its expected value and a conditional-value-at-risk (CVaR) term, thereby discouraging solutions that perform satisfactorily on average but produce excessive shortage, early material accumulation, or tardiness under adverse scenarios. All operational feasibility constraints are imposed separately for each scenario, while non-anticipativity constraints ensure that immediate decisions do not depend on information that is not yet available.

### 4.2. Compact notation and formulation

Let S, C, P, V, M, T, R, and Ω denote suppliers, consolidation centers, projects, 3PL providers, materials, periods, routes, and scenarios. The principal scenario-dependent variables are direct dispatch x, supplier-to-center dispatch y, center-to-site dispatch z, physical arrivals, center and site inventories, backlog B, congestion Q, and binary option variables. Complete notation is reported in Supplementary Tables S1–S3.

For scenario ω, $Z_1^{\omega}$, $Z_2^{\omega}$, $Z_3^{\omega}$, and $Z_4^{\omega}$ denote logistics cost, weighted delivery deviation, site congestion, and transportation emissions. The compact formulation below retains the essential expected-value, CVaR, flow, capacity, carbon, non-anticipativity, and commitment relations; full component expansions and all domain constraints appear in Supplementary Eqs. (S1)–(S62).

$$\min\left(\bar{Z}_1, \tilde{Z}_2, \bar{Z}_3, \bar{Z}_4\right) \tag{15}$$

$$\bar{Z}_j = \sum_{\omega \in \Omega} \pi_\omega Z_j^{\omega}, \qquad j \in \{1,3,4\}. \tag{16}$$

$$\tilde{Z}_2 = \sum_{\omega \in \Omega} \pi_\omega Z_2^{\omega} + \lambda_R \left[\eta + \frac{1}{1-\alpha} \sum_{\omega \in \Omega} \pi_\omega \xi_\omega\right]. \tag{17}$$

$$\xi_\omega \geq Z_2^{\omega} - \eta, \qquad \forall \omega \in \Omega. \tag{18}$$

$$\sum_{p \in P} \sum_{v \in V} \sum_{r \in R} x_{spmvrt}^{\omega} + \sum_{c \in C} \sum_{v \in V} \sum_{r \in R} y_{scmvrt}^{\omega} \leq Cap_{smt}^{S,\omega}, \quad \forall s \in S, m \in M, t \in T, \omega \in \Omega. \tag{19}$$

$$\bar{x}_{spmvrt}^{\omega} = IA_{spmvrt}^{SP,\omega} + \sum_{\tau \in T} \delta_{spvr\tau t}^{SP,\omega} x_{spmvr\tau}^{\omega}, \quad \forall s \in S, p \in P, m \in M, v \in V, r \in R, t \in T, \omega \in \Omega. \tag{20}$$

$$I_{cmt}^{C,\omega} = I_{cm,t-1}^{C,\omega} + \sum_{s \in S} \sum_{v \in V} \sum_{r \in R} \bar{y}_{scmvrt}^{\omega} - \sum_{p \in P} \sum_{v \in V} \sum_{r \in R} z_{cpmvrt}^{\omega}, \quad \forall c \in C, m \in M, t \in T, \omega \in \Omega. \tag{21}$$

$$I_{pmt}^{P,\omega} - B_{pmt}^{\omega} = I_{pm,t-1}^{P,\omega} - B_{pm,t-1}^{\omega} + \sum_{s,v,r} \bar{x}_{spmvrt}^{\omega} + \sum_{c,v,r} \bar{z}_{cpmvrt}^{\omega} - D_{pmt}^{\omega}, \quad \forall p \in P, m \in M, t \in T, \omega \in \Omega. \tag{22}$$

$$\sum_{m \in M} I_{pmt}^{P,\omega} \leq Cap_{pt}^{P}, \quad \forall p \in P, t \in T, \omega \in \Omega. \tag{23}$$

$$\sum_{s \in S} \sum_{m \in M} \sum_{v \in V} \sum_{r \in R} \bar{x}_{spmvrt}^{\omega} + \sum_{c \in C} \sum_{m \in M} \sum_{v \in V} \sum_{r \in R} \bar{z}_{cpmvrt}^{\omega} \leq UCap_{pt}^{\omega} Open_{pt}^{\omega}, \quad \forall p \in P, t \in T, \omega \in \Omega. \tag{24}$$

$$\sum_{s,p,m,r} x_{spmvrt}^{\omega} + \sum_{s,c,m,r} y_{scmvrt}^{\omega} + \sum_{c,p,m,r} z_{cpmvrt}^{\omega} \leq Cap_{vt}^{V,\omega}, \quad \forall v \in V, t \in T, \omega \in \Omega. \tag{25}$$

$$Z_4^{\omega} \leq Cap^{CO_2}, \quad \forall \omega \in \Omega. \tag{26}$$

$$x_{spmvrt}^{\omega} = x_{spmvrt}^{\omega'}, \quad \forall s \in S, p \in P, m \in M, v \in V, r \in R, t \in T^R, \omega, \omega' \in \Omega. \tag{27}$$

$$x_{spmvrt}^{\omega} = \hat{x}_{spmvrt}, \quad \forall s \in S, p \in P, m \in M, v \in V, r \in R, t \in T^F, \omega \in \Omega. \tag{28}$$

Equations (15)–(18) define the multi-objective and risk treatment. Equations (19)–(25) represent supplier capacity, dispatch-to-arrival mapping, inventory/backlog conservation, site receiving and storage, and 3PL capacity. Equation (26) enforces the carbon cap. Equation (27) illustrates immediate-period non-anticipativity, and Eq. (28) fixes implemented decisions. The analogous relations for all transportation stages and binary variables are provided in the Supplementary Material.

## 5. Solution Methodology

This section presents the solution methodology developed for solving the proposed multi-objective mixed-integer linear programming model. The considered problem is computationally challenging because it simultaneously includes supplier assignment, 3PL provider selection, route selection, consolidation center usage, delivery timing, site inventory control, shortage prevention, congestion control, and carbon emission reduction. In addition, the problem has a dynamic nature because BIM–IoT data continuously update material demand, site readiness, logistics availability, and delivery priorities through the digital twin environment.

To solve the proposed problem in a structured and computationally efficient way, a digital-twin-based solution procedure is developed. The methodology integrates periodic and event-triggered parameter updating, multi-objective treatment, exact optimization for sufficiently small instances, and ERH-NSGA-II for larger-scale solution. The final output is a compromise delivery plan that supports the 4PL provider in balancing cost efficiency, just-in-time delivery, site-space feasibility, and carbon performance.

### 5.1. Uncertainty-aware rolling-horizon solution procedure

The proposed solution procedure combines digital-twin state updating with scenario-based rolling-horizon optimization. At each update epoch, the current state is synchronized using the most recent validated observations. A set of future uncertainty scenarios is then constructed for the remaining planning horizon. Previously implemented decisions are fixed, immediate decisions are constrained to be identical across scenarios, and future decisions are treated as scenario-dependent recourse decisions.

The uncertainty-aware multi-objective model is solved using the expected cost, expected congestion, expected carbon emissions, and risk-adjusted delivery-deviation objectives. Only the immediate non-anticipative decisions are implemented. Future scenario-dependent decisions are retained as contingency plans and are recalculated when the next update epoch is reached or when a significant event triggers an earlier replanning cycle.

At each scheduled or event-triggered update epoch, the digital-twin procedure performs the following operations. First, the most recent planning and operational observations are collected and validated. Second, the physical-system state is synchronized with the digital representation. Third, the updated activity-progress forecast is used to calculate $D_{\mathrm{pmt}}$ through Eq. (1). Fourth, the criticality, projected-shortage, and predicted-lateness components are calculated through Eqs. (3)–(5), and $Pr_{\mathrm{pmt}}$ is updated through Eq. (2). Fifth, the remaining operational parameters, including site availability, storage occupancy, unloading capacity, supplier capacity, and logistics-provider capacity, are updated. Finally, the optimization model is solved.

The updated values remain fixed during an individual optimization run. After the immediate-period decisions are implemented, the digital twin continues to observe the physical system. A new solution cycle is initiated at the next scheduled review point or when an operational deviation exceeds its predefined threshold. Implemented decisions are retained, whereas decisions associated with the remaining planning horizon may be revised.

The resulting delivery plan determines the quantity of each material to be shipped, the supplier from which the material is sourced, the 3PL provider assigned to each shipment, the route selected for transportation, the use of consolidation centers, and the timing of delivery to each construction site. Once the first-period decisions are implemented, the digital twin continues to monitor the physical system. If significant deviations are detected, the adaptive resequencing mechanism is activated and the model is updated for the remaining planning horizon.

The general procedure consists of the following steps. First, BIM-based material requirements and project activity information are extracted. Second, IoT-based operational data are collected from vehicles, shipments, and construction sites. Third, the digital twin state is updated and the model parameters are revised. Fourth, the multi-objective optimization model is solved. Fifth, supplier assignments, 3PL assignments, route selections, shipment quantities, and delivery schedules are produced. Sixth, the immediate-period decisions are implemented. Seventh, actual execution is monitored through IoT data. Finally, if deviations exceed predefined thresholds, adaptive resequencing is activated and the planning horizon is updated until all material demands are satisfied.

| **Algorithm 1**. Digital-twin-based uncertainty-aware rolling-horizon procedure |
|---|
| **Input:** Baseline BIM and planning information; current validated digital-twin state; current logistics plan; implemented and committed decisions. |
| **Step 1:** Identify the current update epoch and the remaining planning horizon.<br>**Step 2:** Collect, validate, and synchronize the most recent operational observations.<br>**Step 3:** Calculate the updated nominal demand, priority, site, supplier, shipment, and logistics-capacity parameters.<br>**Step 4:** Construct or revise the uncertainty scenarios for the remaining horizon.<br>**Step 5:** Assign a weight or probability to each scenario.<br>**Step 6:** Fix previously implemented and irrevocably committed decisions.<br>**Step 7:** Define immediate non-anticipative decisions and future scenario-dependent recourse decisions.<br>**Step 8:** Solve the uncertainty-aware multi-objective model.<br>**Step 9:** Obtain the non-dominated solution set and select the preferred compromise solution.<br>**Step 10:** Implement only the immediate common decisions.<br>**Step 11:** Retain future scenario-dependent decisions as contingency plans.<br>**Step 12:** Observe the execution results and update the digital-twin state.<br>**Step 13:** Repeat the procedure at the next scheduled review point or event trigger. |

### 5.2. Multi-objective treatment and exact optimization

The proposed model includes four conflicting objectives: total logistics cost, just-in-time delivery deviation, site congestion, and transportation-related carbon emissions. These objectives have different units and magnitudes; therefore, they must be normalized before comparison or compromise solution selection. For each objective $Z_k$, where (k=1,2,3,4), the normalized value is calculated using Eq. (29).

$$\bar{Z}_k = \frac{Z_k - Z_k^{min}}{Z_k^{max} - Z_k^{min}} \tag{29}$$

where $Z_k^{min}$ and $Z_k^{max}$ represent the best and worst observed values of objective $k$ among the identified feasible solutions. The normalized values obtained from Eq. (29) allow all objectives to be evaluated on a comparable scale.

After obtaining candidate solutions, the final compromise solution is selected using the normalized preference score defined in Eq. (30).

$$score = \alpha_1 \bar{Z}_1 + \alpha_2 \bar{Z}_2 + \alpha_3 \bar{Z}_3 + \alpha_4 \bar{Z}_4 \tag{30}$$

where $\alpha_1$, $\alpha_2$, $\alpha_3$, and $\alpha_4$ represent the relative importance of logistics cost, delivery deviation, site congestion, and carbon emissions, respectively. The base-case values of these weights are specified in the computational implementation section.

This weighting scheme reflects a balanced policy in which logistics cost and delivery reliability receive slightly higher importance, while site-space feasibility and carbon emissions are also explicitly considered. The solution with the lowest value of Eq. (30) among the non-dominated solutions is selected as the final compromise solution for implementation.

For sufficiently small instances, the proposed mathematical model is solved using an exact mixed-integer linear programming solver. In this case, the normalized preference score in Eq. (30) is used to transform the multi-objective model into a scalarized model. This allows the solver to identify an optimal compromise solution under the specified weights. The exact solution is useful for validating the mathematical formulation and for comparing the quality of heuristic solutions. However, as the problem size increases, the number of binary decision variables grows rapidly, especially those related to supplier selection, 3PL assignment, route feasibility, and consolidation center usage. Therefore, exact optimization may become computationally expensive for large-scale practical instances.

### 5.3. Event-Aware Rolling-Horizon NSGA-II

For large-scale instances, an Event-Aware Rolling-Horizon Non-Dominated Sorting Genetic Algorithm II, hereafter referred to as ERH-NSGA-II, is developed to solve the uncertainty-aware multi-objective model presented in Section 4. The method retains the non-dominated sorting, crowding-distance calculation, binary tournament selection, and elitist environmental-selection mechanisms of conventional NSGA-II. These standard mechanisms provide the multi-objective selection backbone and are not claimed as methodological innovations. The problem-specific contribution of ERH-NSGA-II lies in its two-stage scenario-linked chromosome, rolling-horizon warm start, event-affected search mechanism, block-based crossover, priority- and risk-guided adaptive mutation, and hierarchical scenario-feasibility repair procedure.

The algorithm operates at each scheduled or event-triggered digital-twin update epoch. Decisions that have already been implemented or irrevocably committed are fixed at their observed values. Decisions for the immediate non-anticipative periods are required to remain common across all uncertainty scenarios, whereas decisions for later adaptive periods may differ by scenario and represent recourse actions. The algorithm evaluates every candidate delivery policy under all scenarios and returns a non-dominated set that balances probability-weighted logistics cost, risk-adjusted delivery deviation, probability-weighted site congestion, and probability-weighted transportation-related carbon emissions.

#### 5.3.1. Additional algorithmic notation

Table 4 summarizes the additional notation used in ERH-NSGA-II. The logistics sets, parameters, and decision variables retain the definitions introduced in Sections 4.2 and 4.3.

Table 4. Additional notation used in ERH-NSGA-II

| Symbol | Definition |
|---|---|
| $k$ | Current digital-twin update epoch. |
| $\chi$ | A complete chromosome representing a rolling-horizon material-delivery policy. |
| $\chi^c$ | Common chromosome block for immediate non-anticipative periods. |
| $\chi^\omega$ | Scenario-dependent recourse block for scenario $\omega$. |
| $g$ | Index of a chromosome gene. |
| $M_g^{(k)}$ | Binary mask indicating whether gene $g$ is affected at update epoch $k$. |
| $P_0^{(k)}$ | Initial population at update epoch $k$. |
| $P_{\text{carry}}^{(k)}$ | Repaired and horizon-shifted solutions inherited from the preceding Pareto set. |
| $P_{\text{heur}}^{(k)}$ | Population component created by problem-specific heuristic rules. |
| $P_{\text{rand}}^{(k)}$ | Random population component used to preserve diversity. |
| $B_{pm}$ | Decision block containing the genes associated with site $p$ and material $m$. |
| $p_g^{\text{mut}}$ | Adaptive mutation probability assigned to gene $g$. |
| $p_{\min}, p_{\max}$ | Minimum and maximum allowable mutation probabilities. |
| $\widetilde{Pr}_g$ | Normalized delivery-priority value associated with gene $g$. |
| $\text{Risk}_g$ | Scenario-weighted normalized risk score associated with gene $g$. |
| $\beta_P, \beta_R, \beta_M$ | Non-negative coefficients controlling the effects of priority, risk, and event impact on mutation. |
| $Q$ | Set of constraint groups considered in residual-violation measurement. |
| $V_q^\omega(\chi)$ | Normalized residual violation of constraint group $q$ under scenario $\omega$. |
| $\gamma_q$ | Relative severity coefficient of constraint group $q$. |
| $\Lambda_j$ | Penalty coefficient associated with objective $j$. |

#### 5.3.2. Two-stage scenario-linked chromosome representation

Each chromosome represents a complete rolling-horizon material-delivery policy for the remaining planning horizon. Implemented and irrevocably committed decisions are excluded from the chromosome because they are fixed before the evolutionary search begins. The encoded portion contains a common block for the immediate non-anticipative periods and one recourse block for each uncertainty scenario:

$$\chi = [\chi^C, \chi^{\omega_1}, \chi^{\omega_2}, \dots, \chi^{\omega_{|\Omega|}}] \quad (31)$$

In Eq. (31), $\chi^C$ contains the decisions associated with periods in $T^R$, whereas $\chi^{\omega}$ contains the adaptive decisions associated with periods in $T^A$ under scenario $\omega$. The common block is decoded identically under every scenario; therefore, the non-anticipativity requirement for immediate decisions is satisfied by construction rather than by relying only on a posterior repair operation.

For each material requirement, the corresponding gene contains the principal discrete logistics decisions:

$$\mathrm{Gene}_{pmt}^{\omega} = [\mathrm{Sup}_{pmt}^{\omega}, \mathrm{Mode}_{pmt}^{\omega}, \mathrm{CC}_{pmt}^{\omega}, \mathrm{LSP}_{pmt}^{\omega}, \mathrm{Route}_{pmt}^{\omega}, \mathrm{Period}_{pmt}^{\omega}] \quad (32)$$

In Eq. (32), $\mathrm{Sup}_{pmt}^{\omega}$ identifies the selected supplier, $\mathrm{Mode}_{pmt}^{\omega}$ indicates direct or consolidation-based delivery, $\mathrm{CC}_{pmt}^{\omega}$ identifies the selected consolidation center when indirect delivery is used, $\mathrm{LSP}_{pmt}^{\omega}$ identifies the selected 3PL provider, $\mathrm{Route}_{pmt}^{\omega}$ identifies the selected route, and $\mathrm{Period}_{pmt}^{\omega}$ identifies the dispatch period. For periods in $T^R$, the scenario superscript is omitted because the corresponding values are stored once in $\chi^C$ and are common to all scenarios.

The continuous shipment quantities are not independently encoded. During chromosome decoding, they are derived from the scenario-dependent material demand, available inventory, confirmed inbound shipments, supplier capacity, 3PL capacity, consolidation-center capacity, site unloading capacity, storage capacity, transportation lag, and final demand-fulfilment requirements. This representation reduces chromosome dimensionality and avoids arbitrary continuous flows that are inconsistent with the encoded supplier, delivery-mode, route, and timing decisions.

### 5.3.3. Scenario-based chromosome decoding

Chromosome decoding proceeds chronologically over the active rolling horizon. Implemented and committed shipments are first inserted into the delivery state. The common genes are then decoded once and copied to all scenarios. Finally, each scenario-dependent recourse block is decoded using the corresponding demand, transportation-lag, route-availability, site-availability, and resource-capacity parameters.

For each scenario, decoding performs the following sequence. First, the beginning inventories, backlogs, and in-transit quantities are initialized from the synchronized digital-twin state. Second, the decoder reads the supplier, mode, consolidation-center, 3PL, route, and dispatch-period attributes of each common gene. Third, scenario-dependent arrival periods are calculated from the selected dispatch periods and transportation lags. Fourth, direct and consolidation-based material flows are allocated without exceeding the currently available capacities. Fifth, consolidation-center and site inventories are updated period by period. Sixth, the scenario-specific recourse genes are decoded. Seventh, shortages, site congestion, delivery deviation, logistics cost, and carbon emissions are calculated. Finally, any remaining infeasibility is processed through the hierarchical repair mechanism described in Section 5.3.8.

When several material requirements compete for the same limited resource, the decoder gives precedence to requirements with larger delivery-priority values, earlier required-availability periods, and higher projected shortage risk. Ties are resolved using a consistent secondary rule, such as lower incremental cost or lower incremental emissions. The same tie-breaking rule is applied to all comparison runs so that algorithmic performance is not affected by inconsistent decoding choices.

### 5.3.4. Rolling-horizon warm-start initialization

Conventional NSGA-II generally creates a new population independently for each optimization run. In contrast, ERH-NSGA-II reuses valid information from the non-dominated solutions obtained at the preceding digital-twin update epoch. Each inherited solution is shifted to the new planning horizon, genes corresponding to implemented decisions are removed, committed decisions are fixed, expired recourse periods are discarded, and the remaining genes are revalidated against the updated digital-twin state and the revised uncertainty scenarios.

The initial population is constructed as:

$$P_0^{(k)} = P_{\mathrm{carry}}^{(k)} \cup P_{\mathrm{heur}}^{(k)} \cup P_{\mathrm{rand}}^{(k)} \quad (33)$$

In Eq. (33), $P_{\mathrm{carry}}^{(k)}$ contains inherited and repaired solutions, $P_{\mathrm{heur}}^{(k)}$ contains newly created heuristic solutions, and $P_{\mathrm{rand}}^{(k)}$ contains randomly created feasible or repairable solutions. Duplicate chromosomes are removed before the first fitness evaluation. If the inherited component is smaller than required because many previous solutions become infeasible, the missing positions are filled by heuristic and random chromosomes.

The heuristic component uses cost-oriented, distance-oriented, carbon-oriented, just-in-time-oriented, consolidation-oriented, reliability-oriented, and continuity-oriented construction rules. The reliability-oriented rule prioritizes assignments that remain feasible across a larger proportion of scenarios. The continuity-oriented rule preserves unaffected assignments from the most recently selected plan and changes only decisions that conflict with the updated state. The random component preserves search diversity and limits excessive convergence around the preceding Pareto front when the new event substantially changes the feasible region.

### 5.3.5. Event-affected gene mask

A newly detected event does not necessarily affect every decision in the chromosome. ERH-NSGA-II therefore constructs an affected-gene mask by tracing each changed digital-twin state variable to the related sites, materials, suppliers, 3PL providers, consolidation centers, routes, and periods. The mask is defined in Eq. (34) as:

$$M_g^{(k)} = \begin{cases} 1, & \text{if gene } g \text{ is affected by the updated state or event at epoch } k \\ 0, & \text{otherwise.} \end{cases} \quad (34)$$

Genes with $M_g^{(k)} = 1$ receive increased probabilities of crossover participation, mutation, and targeted repair. Genes with $M_g^{(k)} = 0$ are preferentially preserved when they remain feasible. This mechanism focuses the search on the portion of the delivery policy that requires revision while limiting unnecessary disruption to unaffected decisions. Table 5 summarizes the mapping between digital-twin events and affected chromosome components.

Table 5. Mapping between digital-twin events and affected chromosome components

| Event category | Principal affected chromosome components |
|---|---|
| Project-progress or demand update | Material, site, priority, quantity allocation, and delivery period. |
| Site closure or unloading-capacity reduction | Site, period, delivery mode, consolidation center, and route. |
| Supplier disruption | Supplier, delivery mode, period, and quantity allocation. |
| 3PL-capacity disruption | 3PL provider, route, period, and quantity allocation. |
| Route disruption or travel-time change | Route, 3PL provider, dispatch period, and expected arrival period. |
| Shipment delay | Dispatch/arrival timing, route, 3PL provider, and confirmed inbound availability. |
| Inventory discrepancy | Quantity allocation, delivery mode, consolidation decision, and period. |
| Carbon-restriction change | 3PL provider, route, delivery mode, and consolidation decision. |
| Data-quality event | Parameters and genes linked to the uncertain or missing observation. |

The site–material block crossover exchanges coherent supplier, mode, provider, route, and dispatch decisions, while adaptive mutation increases search pressure for high-priority, high-risk, and event-affected genes. The exact operator equations and additional notation are reported in Supplementary Section S2.

#### 5.3.8. Hierarchical scenario-feasibility repair

After initialization, crossover, and mutation, each chromosome is processed by a hierarchical repair procedure. The repair order reflects the logical dependency among rolling-horizon commitments, non-anticipativity, network feasibility, resource capacities, inventory balance, and environmental restrictions. A lower-level condition is not repaired before the higher-level requirements on which it depends have been restored.

The repair procedure contains nine levels. Level 1 restores implemented and irrevocably committed decisions to their fixed observed values. Level 2 restores non-anticipativity by making all immediate-period decisions identical across scenarios. When the scenario blocks contain inconsistent immediate decisions, the common value is selected using feasibility, scenario coverage, and weighted objective deterioration. Level 3 restores route and receiving feasibility by replacing unavailable routes, closed-site periods, or infeasible receiving options with the nearest admissible alternatives. When direct delivery is infeasible, consolidation-based delivery is considered when allowed by the network.

Level 4 resolves supplier-capacity violations by transferring excess assignments to feasible alternative suppliers or shifting non-urgent dispatches to admissible periods. Level 5 resolves 3PL-capacity violations by replacing overloaded providers, changing routes, splitting eligible material flows, or shifting lower-priority shipments. Level 6 repairs consolidation-center capacity by reassigning flows to alternative centers, selecting direct delivery where feasible, or shifting inbound and outbound flows while preserving material continuity. Level 7 repairs site unloading and storage violations by postponing, splitting, rerouting, or consolidating arrivals. Level 8 recalculates shipment quantities and arrivals to restore dispatch-arrival consistency, inventory balance, backlog accounting, and terminal demand fulfilment. Shortage is retained only when it cannot be removed without violating a higher-level restriction. Level 9 restores carbon feasibility by replacing high-emission 3PL-route combinations, increasing shipment consolidation, or reallocating eligible flows to lower-emission alternatives without violating the preceding repair levels.

When the hierarchical procedure cannot fully restore feasibility, the remaining violation is quantified as:

$$V(\chi) = \sum_{\omega \in \Omega} \pi_\omega \sum_{q \in Q} \gamma_q V_q^\omega(\chi) \qquad (35)$$

The corresponding penalized objective value is:

$$\hat{Z}_j(\chi) = Z_j(\chi) + \Lambda_j V(\chi), \qquad j = 1,2,3,4 \qquad (36)$$

In Eq. (35), $V_q^\omega(\chi)$ is the normalized residual violation of constraint group $q$ under scenario $\omega$, and $\gamma_q$ represents the relative severity of that constraint group. Equation (36) discourages residual infeasibility through objective-specific penalty coefficient $\Lambda_j$. Feasible solutions have $V(\chi) = 0$ and are therefore evaluated without a penalty.

#### 5.3.9. Fitness evaluation, selection, and termination

Every repaired chromosome is decoded under all uncertainty scenarios. The evaluation procedure uses the objective functions defined in Section 4 to calculate probability-weighted logistics cost, risk-adjusted delivery deviation, probability-weighted site congestion, and probability-weighted carbon emissions. The delivery-risk component is calculated from the scenario-specific delivery-deviation values using the CVaR formulation. The same scenario set and scenario weights are used for all chromosomes within one update epoch.

After objective evaluation, solutions are ranked using non-dominated sorting. The first front contains solutions that are not dominated by any other member of the population. Crowding distance is calculated within each front to preserve objective-space diversity. Binary tournament selection prefers lower non-domination rank and, when ranks are equal, larger crowding distance. Parent and offspring populations are combined, and elitist environmental selection retains the best population according to rank and crowding distance. These operations follow conventional NSGA-II and are deliberately separated from the problem-specific operators introduced above.

The algorithm terminates when the maximum generation limit is reached, the computational-time limit is reached, or the improvement of the non-dominated front remains below a predefined tolerance for a specified number of consecutive generations. The comparison algorithms must use an equivalent computational budget and common stopping rules. The population size, operator probabilities, penalty coefficients, stopping limits, and other numerical settings are reported in the computational-implementation section rather than embedded in the general algorithm description.

### 5.3.10. Complete ERH-NSGA-II procedure

Algorithm 2 presents the complete ERH-NSGA-II procedure used to solve the uncertainty-aware rolling-horizon material-delivery problem. At each digital-twin update, implemented decisions are fixed, the remaining horizon is divided into immediate non-anticipative and scenario-dependent recourse periods, and event-affected decision variables are identified. The initial population combines repaired solutions inherited from the previous Pareto set with heuristic and random solutions. Each chromosome is decoded and evaluated under all uncertainty scenarios, followed by non-dominated sorting, block crossover, priority- and risk-guided mutation, and hierarchical feasibility repair. The algorithm returns a non-dominated set of delivery policies, implements only the immediate common decisions, and retains future scenario-dependent decisions as contingency plans.

Algorithm 2. Event-Aware Rolling-Horizon NSGA-II

| Item | Procedure |
|---|---|
| **Input** | Current validated digital-twin state; remaining planning horizon; uncertainty scenarios and scenario weights; implemented and committed decisions; and the preceding non-dominated solution set, when available. |
| **Output** | Final non-dominated delivery-policy set, selected compromise solution, immediate common decisions, and scenario-dependent contingency decisions. |
| 1 | Identify the current update epoch and fix all implemented and irrevocably committed decisions. |
| 2 | Divide the remaining horizon into immediate non-anticipative periods $T^R$ and adaptive recourse periods $T^A$. |
| 3 | Construct the affected-gene mask $M_g^{(k)}$ from the synchronized digital-twin changes. |
| 4 | Shift, truncate, revalidate, and repair valid solutions inherited from the preceding Pareto set. |
| 5 | Create additional chromosomes using heuristic and random initialization rules. |
| 6 | Form $P_0^{(k)}$ by combining inherited, heuristic, and random solutions; remove duplicates and restore the required population size. |
| 7 | Decode every chromosome: insert committed decisions, decode the common block, calculate dispatch and scenario-dependent arrival periods, decode each recourse block, and update inventories and backlogs. |
| 8 | Apply hierarchical scenario-feasibility repair and calculate the four uncertainty-aware objective values. |
| 9 | Perform non-dominated sorting and calculate crowding distances. |
| 10 | Select parent chromosomes using binary tournament selection. |
| 11 | Apply site-material block crossover while preserving committed decisions and common-block consistency. |
| 12 | Calculate $p_g^{\mathrm{mut}}$ for each eligible gene and apply priority- and risk-guided mutation. |
| 13 | Restore implemented decisions and non-anticipativity, then apply the hierarchical repair procedure to every offspring chromosome. |
| 14 | Decode and evaluate the offspring under all scenarios. |
| 15 | Combine parent and offspring populations and select the next generation using non-domination rank and crowding distance. |
| 16 | Repeat Steps 10-15 until a stopping condition is satisfied. |
| 17 | Return the final non-dominated set and select the preferred compromise solution using the solution-selection rule defined in Section 5.2. |
| 18 | Implement only the immediate common decisions and retain the scenario-dependent recourse decisions as contingency plans. |
| 19 | Store the current Pareto set for warm-start initialization at the next digital-twin update epoch. |

The distinction between ERH-NSGA-II and conventional NSGA-II lies in the two-stage scenario-linked chromosome, rolling-horizon Pareto warm start, affected-gene mask, block-based crossover, adaptive mutation, and hierarchical scenario-feasibility repair. The standard sorting, crowding-distance, tournament-selection, and elitist-selection procedures are retained solely as the multi-objective evolutionary backbone. The contribution of each problem-specific component should be evaluated through the ablation and benchmark experiments reported in the computational-results section.

## 5.4. Performance evaluation indicators

The performance of the proposed solution methodology is evaluated using operational, temporal, spatial, environmental, and computational indicators. The operational indicator is total logistics cost, including transportation cost, handling cost, consolidation cost, inventory cost, and penalty cost. The temporal indicator is delivery deviation, which reflects early and late material availability at construction sites. The spatial indicator is site congestion, measured based on the amount of site inventory exceeding the preferred safe storage level. The environmental indicator is total transportation-related carbon emissions.

Additional performance indicators include on-time delivery rate, 3PL utilization, consolidation center utilization, number of adaptive resequencing actions, average site inventory level, number of site capacity violations, and computational time. These indicators provide a comprehensive basis for evaluating the effectiveness of the proposed BIM–IoT-driven digital twin-based 4PL solution approach.

The proposed methodology enables the 4PL provider to evaluate trade-offs among cost efficiency, delivery reliability, site feasibility, and environmental sustainability. It also supports adaptive logistics control by updating delivery decisions in response to real-time deviations captured through the digital twin.

# 6. Case Study and Computational Experimental Design

## 6.1. Application setting

The framework is evaluated for a multi-site Iranian steel-construction logistics network with five suppliers, four consolidation centers, five 3PL providers, six projects, and a 12-week weekly rolling horizon. The 4PL control tower coordinates direct and consolidation-based deliveries while considering project progress, storage and unloading limits, route distance, provider capacity, and emissions.

Four case-policy configurations isolate decentralized planning (S1), coordinated cost-focused 4PL planning (S2), BIM–IoT digital-twin updating and JIT control (S3), and the complete uncertainty- and carbon-aware policy (S4). Events include progress delay or acceleration, temporary receiving-capacity reduction, and long-distance transport delay. Table 6 summarizes the condensed application and benchmark design.

Table 6. Condensed application and benchmark design

| Design element | Implemented setting |
|---|---|
| Case network | 5 suppliers; 4 consolidation centers; 5 3PLs; 6 sites; 5 materials; 12 weekly periods. |

| | |
|---|---|
| Policy comparison | S1 decentralized; S2 coordinated cost-focused; S3 digital-twin JIT; S4 full carbon- and uncertainty-aware. |
| Benchmark suite | S1–S2 small, M1–M2 medium, C1–C2 case-sized, L1–L2 large. |
| Scenario dimensions | 3, 4, 5, and 7 scenarios from small to large classes. |
| Comparison methods | Exact scalarized MILP (small only), NSGA-II, MOEA/D, NSGA-III, ERH-NSGA-II. |
| Replications | 30 independent seeds per algorithm–instance combination; matched seeds for ablation. |
| Primary indicators | Normalized hypervolume, IGD+, additive epsilon, feasibility, runtime, and exact scalarized gap. |

### 6.2. Computational settings and protocol

All evolutionary methods used common instance/scenario sets, feasibility calculations, population and generation budgets within each size class, and the same 30-seed list. The pooled non-dominated union was used as the reference front where a true front was unavailable. Friedman tests, Holm-adjusted Wilcoxon comparisons, and Vargha–Delaney dominance probabilities were evaluated at the 5% level. The principal computational settings and benchmark-instance characteristics are reported in Tables 7 and 8, respectively.

Table 7. Principal computational settings

| Parameter | Setting |
|---|---|
| Population / generations | 32/50 small; 30/40 medium; 32/45 case-sized; 34/55 large. |
| Crossover / mutation | 0.90 crossover; adaptive mutation 0.01–0.20. |
| Initialization | 35% heuristic new individuals; up to 50% warm-start carry. |
| CVaR | Confidence 0.90; coefficient 0.25. |
| Delivery priority | Prmax=5; λC=0.50, λS=0.30, λL=0.20; fixed ex ante. |
| Exact solver | 120 s; relative MIP gap 0.001. |
| Feasibility restoration | Up to 30 reconstructions with common basic/hierarchical repair budgets. |
| Environment | Python/SciPy-HiGHS benchmark implementation; CPU times compared only within that environment. |

Table 8. Benchmark-instance characteristics

| Instance | Class | S | C | 3PL | P | M | T | Ω | Chr. |
|---|---|---|---|---|---|---|---|---|---|
| S1 | Small | 3 | 1 | 3 | 2 | 3 | 5 | 3 | 18 |
| S2 | Small | 3 | 1 | 3 | 2 | 3 | 5 | 3 | 18 |
| M1 | Medium | 5 | 3 | 4 | 4 | 4 | 8 | 4 | 49 |
| M2 | Medium | 5 | 3 | 4 | 4 | 4 | 8 | 4 | 52 |
| C1 | Case-sized | 5 | 4 | 5 | 6 | 5 | 12 | 5 | 114 |
| C2 | Case-sized | 5 | 4 | 5 | 6 | 5 | 12 | 5 | 122 |
| L1 | Large | 7 | 4 | 6 | 8 | 6 | 12 | 7 | 258 |
| L2 | Large | 7 | 4 | 6 | 8 | 6 | 12 | 7 | 270 |

The benchmark design preserves the supplier–consolidation-center–3PL–site network structure. Supplier capacities are scaled relative to aggregate demand to create both flexible and binding conditions. Site storage and unloading capacities are specified relative to site demand, and transportation alternatives reflect route distance, provider cost, emissions, and reliability. All construction rules, seeds, and numerical settings are reported to support reproducibility. Table 9 summarizes the comparison algorithms and their roles in the evaluation.

Table 9. Comparison algorithms and principal characteristics

| Method | Principal mechanism | Role in comparison |
|---|---|---|
| Exact scalarized MILP | Deterministic equivalent under fixed weights | Small-instance reference |
| NSGA-II | Non-dominated sorting and crowding distance | Conventional evolutionary baseline |
| MOEA/D | Tchebycheff decomposition and neighborhood replacement | Decomposition baseline |
| NSGA-III | Reference-direction association and niching | Many-objective baseline |
| ERH-NSGA-II | Scenario-linked chromosome, warm start, event mask, block/adaptive operators and repair | Proposed method |

Conventional NSGA-II used random initialization, gene-level crossover, standard mutation, non-dominated sorting, crowding distance, and basic feasibility correction. MOEA/D used Tchebycheff decomposition with neighborhood replacement. NSGA-III used reference-direction association and niching. ERH-NSGA-II used the two-stage scenario-linked representation and the event-responsive components described in Section 5.3. Standard non-dominated sorting and crowding distance are retained as selection mechanisms and are not claimed as novel. The detailed numerical settings used in the benchmark experiments are reported in Table 10.

Table 10. Detailed benchmark parameter settings

| Parameter | Implemented setting |
|---|---|
| Master random seed | 20260726 |
| Independent runs | 30 per algorithm–instance combination |
| Population size | 32 small; 30 medium; 32 case-sized; 34 large |
| Generations | 50 small; 40 medium; 45 case-sized; 55 large |
| Crossover probability | 0.90 |
| Adaptive mutation range | 0.01–0.20 |
| Heuristic initialization share | 35% of newly created individuals |
| Warm-start carry share | Up to 50% of the initial population |
| CVaR confidence level | 0.90 |
| CVaR coefficient | 0.25 |
| Adaptive mutation coefficients | Priority 0.30; risk 0.35; event mask 0.35 |
| Priority scale upper bound, $Pr_{max}$ | 5.0 |
| Priority-component weights | $\lambda_C = 0.50$; $\lambda_S = 0.30$; $\lambda_L = 0.20$; sum = 1.00 |
| Priority-weight selection | Ex ante managerial policy; fixed across algorithms, instances, scenarios, and seeds |
| Exact-solver budget | 120 s; relative MIP gap 0.001 |
| Final feasibility restoration | Up to 30 reconstruction attempts; 5 basic or 4 hierarchical repair passes; identical completion rule across algorithms |

Within each size class, all evolutionary algorithms used the same population size, generation budget, instance set, scenario set, and 30-seed list. The delivery-priority scale was fixed at $Pr_{max} = 5.0$, with $\lambda_C = 0.50$ for activity criticality, $\lambda_S = 0.30$ for projected shortage, and $\lambda_L = 0.20$ for predicted lateness. The weights sum to one and were specified ex ante as managerial policy weights, reflecting the ordering critical-path protection > shortage prevention > predicted lateness. They were held constant across algorithms, instances, scenarios, and seeds and were not tuned separately for any method. Increased search and repair budgets were used for the large instances, and the same final feasibility-restoration budget was applied to all comparison algorithms. Table S19 summarizes the algorithmic performance indicators.

Detailed supplier, 3PL, project, data-source, policy-scenario, uncertainty-rule, indicator, and ablation tables are reported in Supplementary Section S3.

## 7. Results and Discussion

### 7.1. Case-policy results

Table 11 shows that coordination alone lowers cost and improves delivery performance, while state updating and adaptive JIT control produce the largest reductions in deviation and congestion. Relative to S2, S3 reduces delivery deviation by 36.1% and congestion by 32.2%. The complete S4 policy further reduces deviation to 354 ton-weeks, congestion to 43.8%, and emissions to 342.4 $tCO_2e$, while increasing the on-time rate to 90.6%.

Table 11. Condensed case-policy performance

| Policy | Cost (million IRR) | Deviation | Congestion | $CO_2$ | On-time |
|---|---|---|---|---|---|
| S1 | 18,470 | 812 | 78.4% | 426.5 | 68.7% |
| S2 | 17,125 | 604 | 70.2% | 401.8 | 75.4% |
| S3 | 17,640 | 386 | 47.6% | 383.6 | 88.2% |
| S4 | 18,015 | 354 | 43.8% | 342.4 | 90.6% |

### 7.3. Exact verification on small benchmark instances

The two small instances were solved through the scalarized exact formulation with a 120-s solver limit and a relative MIP gap of 0.001. Table 12 compares the proven exact scalarized score with the mean and standard deviation produced by each evolutionary algorithm over 30 independent seeds. The comparison checks objective calculations and provides a solution-quality reference; it does not constitute an exact multi-objective Pareto-front proof.

Table 12. Exact scalarized verification over 30 independent runs

| Instance | Algorithm | Exact score | Mean algorithm score ± SD | Mean gap ± SD (%) |
|---|---|---|---|---|
| S1 | NSGA-II | 0.1076 | 0.1455 ± 0.0178 | 35.3 ± 16.6 |
| S1 | MOEA/D | 0.1076 | 0.2364 ± 0.0155 | 119.7 ± 14.4 |
| S1 | NSGA-III | 0.1076 | 0.1536 ± 0.0159 | 42.8 ± 14.8 |
| S1 | ERH-NSGA-II | 0.1076 | 0.1121 ± 0.0012 | 4.2 ± 1.1 |
| S2 | NSGA-II | 0.0846 | 0.1260 ± 0.0246 | 48.9 ± 29.1 |
| S2 | MOEA/D | 0.0846 | 0.2521 ± 0.0364 | 198.0 ± 43.1 |
| S2 | NSGA-III | 0.0846 | 0.1351 ± 0.0162 | 59.8 ± 19.1 |
| S2 | ERH-NSGA-II | 0.0846 | 0.0914 ± 0.0023 | 8.1 ± 2.7 |

ERH-NSGA-II produced the smallest mean evolutionary gap for both instances. Its mean gap was 4.2% for S1 and 8.1% for S2, compared with 35.3% and 48.9% for conventional NSGA-II. Relative to conventional NSGA-II, ERH-NSGA-II reduced the mean scalarized gap by approximately 88.2% for S1 and 83.5% for S2. The best ERH-NSGA-II runs were within 1.6% and 1.9% of the exact scalarized scores. These results support close scalarized proximity while avoiding a claim of exact multi-objective optimality.

### 7.2. Verification and comparative performance

On the two small instances, ERH-NSGA-II obtained mean scalarized gaps of 4.2% and 8.1%, versus 35.3% and 48.9% for conventional NSGA-II; its best gaps were 1.6% and 1.9%. Across all four size classes, ERH-NSGA-II achieved the highest normalized hypervolume and lowest IGD+ among the tested methods, with additional runtime. All methods produced fully feasible final populations for all instances, including L1 and L2, over all 30 seeds. Table 13 summarizes the corresponding class-level Pareto performance.

Table 13. Class-level Pareto performance (mean ± SD)

| Class | HV: baseline → ERH | IGD+: baseline → ERH | ERH time |
|---|---|---|---|
| Small | 0.770 → 0.834 | 0.068 → 0.011 | 12.237 s |
| Medium | 0.546 → 0.611 | 0.155 → 0.107 | 16.267 s |
| Case-sized | 0.364 → 0.558 | 0.251 → 0.107 | 27.079 s |
| Large | 0.318 → 0.593 | 0.378 → 0.190 | 55.149 s |

Relative to conventional NSGA-II, ERH-NSGA-II increased hypervolume by 8.4%, 11.8%, 53.4%, and 88.2% and reduced IGD+ by 85.8%, 30.9%, 57.3%, and 49.8% from small to large classes. The Friedman tests rejected equal performance for hypervolume ($p=4.14\times10^{-5}$) and IGD+ ($p=3.31\times10^{-4}$). Table 14 reports the Holm-adjusted paired comparisons and dominance probabilities.

Table 14. Holm-adjusted paired comparisons with ERH-NSGA-II

| Baseline | Holm p (HV / IGD+) | Dominance P (HV / IGD+) |
|---|---|---|
| NSGA-II | 0.0117 / 0.0117 | 0.797 / 0.766 |
| MOEA/D | 0.0117 / 0.0117 | 1.000 / 1.000 |
| NSGA-III | 0.0117 / 0.0117 | 0.797 / 0.766 |

### 7.3. Sensitivity, robustness, and operational thresholds

The one-factor and multi-factor analyses show that the main risks are conditional rather than independent. Demand growth becomes especially damaging when 3PL capacity falls below baseline; consolidation capacity moderates the cost of a tighter carbon cap; and data accuracy has its largest value under high demand. The balanced compromise policy ranked first under combined disturbances, whereas the cost-oriented policy was least robust. Complete response curves, elasticities, interaction models, robustness tables, and figures are provided in Supplementary Section S4.

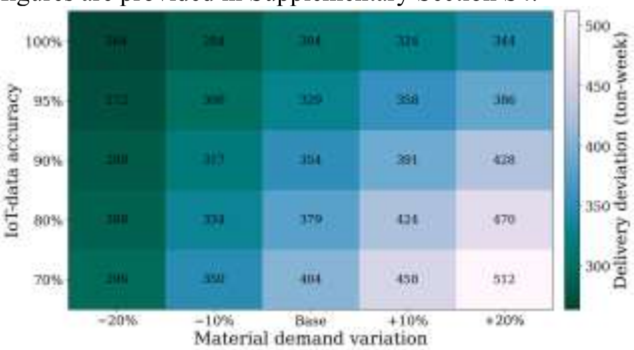


Figure 2. Interaction between material-demand variation and 3PL capacity on delivery-risk CVaR.

Figure 2 shows a pronounced demand–capacity interaction. At 20% demand growth and 20% capacity reduction, delivery-risk CVaR reaches approximately 612 ton-weeks. Increasing capacity by 40 percentage points under the same demand condition reduces CVaR to about 404 ton-weeks. The corresponding reduction is smaller under low demand, confirming that flexible capacity should be concentrated in high-demand periods.

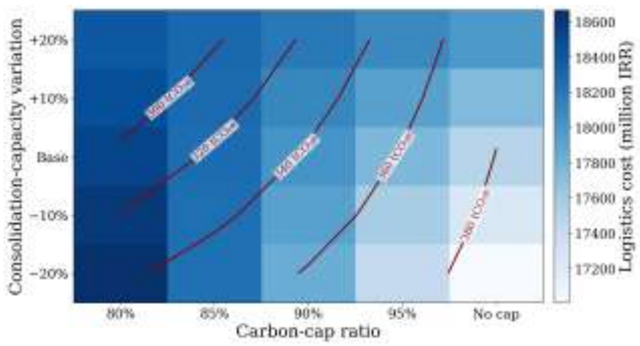


Figure 3. Joint effect of carbon-cap ratio and consolidation capacity on logistics cost, with $CO_2$-emission contours.

Figure 3 demonstrates that consolidation capacity moderates the cost of tighter carbon control. At the 80% carbon-cap ratio, increasing consolidation capacity from −20% to +20% reduces the response-model cost from approximately 18.66 to 18.41 billion IRR while moving the solution toward lower emission contours. Under a loose cap, the cost benefit of extra consolidation is smaller, which supports selective rather than uniform capacity expansion. The estimated operational thresholds and associated control actions are reported in Table 15, while the 30-run event-response ablation results are summarized in Table 16.

Table 15. Estimated operational thresholds and actions

| Control threshold | Operational target | Action |
|---|---|---|
| 3PL capacity < 0.985 | On-time ≥ 90% | Reserve backup capacity. |
| Site storage < 0.928 | Congestion ≤ 50% | Consolidate, split, or postpone arrivals. |
| IoT accuracy < 84.5% | Deviation ≤ 400 ton-weeks | Validate state and shorten update/commitment intervals. |
| Carbon-cap ratio < 0.838 | Cost premium ≤ 5% | Use cleaner routes/providers or authorize a larger premium. |
| Consolidation capacity < 1.033 | Emissions ≤ 340 $tCO_2e$ | Provide temporary capacity or intensify load coordination. |

Table 16. Ablation and event-response results over 30 independent runs

| Variant | Norm. HV | IGD+ | ε | Time (s) | Feasible |
|---|---|---|---|---|---|
| A0 Standard restart | 0.307 ± 0.042 | 0.286 ± 0.048 | 0.363 | 15.283 | 100% |
| A1 Two-stage | 0.293 ± 0.045 | 0.304 ± 0.052 | 0.370 | 15.353 | 100% |
| A2 + warm start | 0.463 ± 0.062 | 0.058 ± 0.031 | 0.199 | 15.004 | 100% |
| A3 + event mask | 0.430 ± 0.021 | 0.091 ± 0.015 | 0.225 | 17.526 | 100% |
| A4 + block/adaptive | 0.428 ± 0.027 | 0.094 ± 0.019 | 0.223 | 17.850 | 100% |
| A5 Full repair | 0.439 ± 0.023 | 0.077 ± 0.013 | 0.254 | 24.981 | 100% |

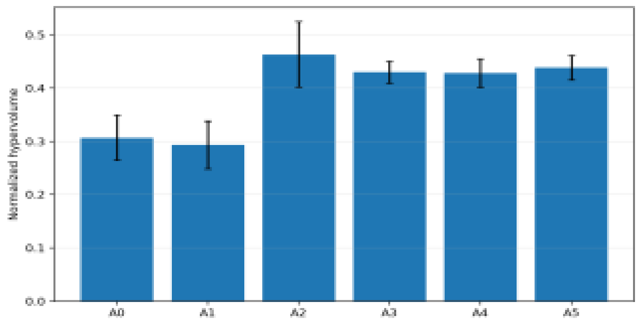


Figure 4. Normalized hypervolume of the ablation variants over 30 independent event-response runs.

As shown in Figure 4, the full A5 method increases normalized hypervolume by approximately 2.0% and reduces IGD+ by approximately 16.0% relative to A3, while its runtime is 63.5% higher than the standard restart. All ablation variants ended with fully feasible populations in every run. The experiment does not imply monotonic benefit from every isolated component; it supports the integrated mechanism in which warm starting supplies reusable search information, the event mask concentrates changes, and the block/adaptive operators and repair procedure manage diversity and feasibility.

### 7.4. Event-response ablation and managerial implications

The 30-run ablation identifies Pareto warm starting as the principal source of rapid recovery after an event: adding warm start increased normalized hypervolume from 0.293 to 0.463 and reduced IGD+ from 0.304 to 0.058. The event mask concentrates search on affected decisions, while block/adaptive operators and hierarchical repair manage diversity and feasibility. Every ablation variant ended with fully feasible populations. Table 17 summarizes the resulting trigger–action rules for 4PL control.

Table 17. Core trigger–action rules for 4PL control

| Trigger | Decision and responsible actor |
|---|---|
| Demand >1.10 and 3PL capacity <1.00 | Protect priority materials and reserve backup capacity (4PL/procurement). |
| Congestion >50% or storage <0.928 | Postpone, split, or redirect non-critical deliveries (site/4PL). |
| IoT accuracy <84.5% | Validate the state and shorten update/commitment windows (DT operator). |
| CVaR >520 ton-weeks | Select a risk-averse policy and activate contingency capacity (project manager/4PL). |
| Route or supplier disruption | Use approved alternatives while retaining implemented commitments (4PL/procurement). |
| Carbon ratio <0.838 without premium approval | Increase consolidation/clean-provider use or revise the target (management/4PL). |

### 7.5. Integrated discussion and limitations

RQ1 is answered by the validated state-to-parameter and feedback architecture; RQ2 by the scenario-based rolling-horizon model with dispatch–arrival mapping, non-anticipativity, recourse, and CVaR; RQ3 by the exact, benchmark, statistical, scalability, and ablation evidence; and RQ4 by the interaction-dependent thresholds and trigger–action rules. The results support the construction-specific integration claimed in the Introduction rather than novelty of the underlying concepts individually.

The decision-rule structure is transferable, but numerical thresholds require local specification. The study evaluates an operational decision architecture computationally rather than a fully deployed cyber-physical system, covers one construction-sector application, and does not provide long-term multi-organization validation of sensor-error and missing-message behavior. Detailed additional evidence is supplied separately to preserve the concise main-paper presentation.

## 8. Conclusion

This study developed an uncertainty-aware BIM–IoT digital-twin framework for 4PL-orchestrated JIT and low-carbon material delivery. The framework converts validated operational observations into updated demand, priority, site, and logistics parameters and links them to a scenario-based rolling-horizon model that separates implemented, immediate non-anticipative, and future recourse decisions.

ERH-NSGA-II combines scenario-linked encoding, Pareto warm start, event-focused search, problem-specific operators, and hierarchical repair. The reported benchmarks show improved Pareto convergence and coverage relative to the tested NSGA-II, MOEA/D, and NSGA-III implementations, while the case analysis and sensitivity experiments identify actionable capacity, site-space, data-quality, consolidation, and carbon-control rules.

The contribution is an operational and computational decision architecture, not a fully deployed industrial digital twin. Future research should examine multi-organization deployment, long-horizon operational data, richer correlated uncertainty, online scenario learning, and decomposition or parallel solution methods for larger networks.

## References


[1] Tetik M, Brusselaers N, Fredriksson A. Conceptual model for aligning construction logistics capacity through simulation. Automation in Construction. 2025;175:106190.

[2] Zaalouk A, Moon S, Han S. Operations planning and scheduling in off-site construction supply chain management: Scope definition and future directions. Automation in Construction. 2023;153:104952.

[3] Jaśkowski P, Sobotka A, Czarnigowska A. Decision model for planning material supply channels in construction. Automation in Construction. 2018;90:235–242.

[4] Golpîra H. Optimal integration of the facility location problem into the multi-project multi-supplier multi-resource construction supply chain network design under the vendor managed inventory strategy. Expert Systems with Applications. 2020;139:112841.

[5] Abdzadeh B, Noori S, Ghannadpour SF. A comprehensive mathematical model for quality integration in a project supply chain with concentrating on material flow and transportation. Advanced Engineering Informatics. 2023;57:102034.

[6] Asadujjaman M, et al. An integrated multi-project scheduling, materials ordering and suppliers selection problem. Procedia Computer Science. 2023;219:1609–1616.

[7] Chen Z, et al. Integrating environmental considerations and resilience in material sourcing for construction projects: A two-stage stochastic programming model. Computers & Industrial Engineering. 2025;204:111027.

[8] Ekeskär A, Rudberg M. Third-party logistics in construction: Perspectives from suppliers and transport service providers. Production Planning & Control. 2022;33(9–10):831–846.

[9] Ekeskär A, Havenvid MI. Third-party logistics providers in construction projects: Implications for coopetitive interaction in forced relationships. Journal of Business & Industrial Marketing. 2025;40(13):171–185.

[10] Le PL, et al. Integrated construction supply chain: An optimal decision-making model with third-party logistics partnership. Construction Management and Economics. 2021;39(2):133–155.

[11] Lara JCF, et al. Pathways toward net-zero emissions in the construction industry: A framework integrating circular economy and Industry 4.0 innovations. Building and Environment. 2025;113652.

[12] Nazzal H. Strategic digital leadership in construction: Overcoming organizational barriers to sustainable competitiveness. International Journal of Industrial Engineering & Production Research. 2025;36(3):71–80.

[13] Zhang W, Kang K, Zhong RY. A cost evaluation model for IoT-enabled prefabricated construction supply chain management. Industrial Management & Data Systems. 2021;121(12):2738–2759.

[14] Metvaei S, et al. Developing a BIM-enabled robotic manufacturing framework to facilitate mass customization of prefabricated buildings. Computers in Industry. 2025;164:104201.

[15] RezaHoseini A, Ghannadpour SF, Noori S, Yazdani M. Analyzing the influence of Building Information Modeling (BIM) on construction project management areas of knowledge: Using a hybrid FANP-FVIKOR approach. International Journal of Industrial Engineering & Production Research. 2019;30(1):57–92.

[16] Rangasamy V, Yang JB. The convergence of BIM, AI and IoT: Reshaping the future of prefabricated construction. Journal of Building Engineering. 2024;84:108606.

[17] Hasheminasab Z, Mazroui Nasrabadi E, Sadeqi-Arani Z. Challenges and drivers of the Internet of Things in the supply chain: A systematic review. International Journal of Industrial Engineering & Production Research. 2024;35(3):63–79.

[18] Islahudin N, Nugroho DS, Arifin Z, Rahadian H, Suprijono H. Real-time scheduling approach in Internet of Things-enabled production monitoring systems. International Journal of Industrial Engineering & Production Research. 2024;35(4):12–28.

[19] Pittri H, Godawatte GAGR, Forster AM. Internet of Things in construction supply chain management: A review of applications, challenges, integration pathways and future directions. Journal of Engineering, Design and Technology. 2026;24(3):666–691.

[20] Li X, Lu W, Xue F, Wu L, Zhao R, Lou J, Xu J. Blockchain-enabled IoT-BIM platform for supply chain management in modular construction. Journal of Construction Engineering and Management. 2022;148(2):0002229.

[21] Zhang X, et al. A review of building digital twins: Framework and enabling technologies. Journal of Building Engineering. 2025;113117.

[22] Li J, Wang J. Digital twin-driven management strategies for logistics transportation systems. Scientific Reports. 2025;15(1):12186.

[23] Lee D, Lee S. Digital twin for supply chain coordination in modular construction. Applied Sciences. 2021;11(13):5909.

[24] Edalatpour MA, Al-e SMJM, Ghasemi S. Harmonizing project management and supply chain for sustainable construction: A comprehensive mathematical model and case study. Sustainable Futures. 2025;100805.

[25] Zhang Y, et al. Green fourth-party logistics network design under carbon cap-and-trade policy. International Journal of Production Economics. 2025;282:109540.

[26] Putra HD, Sriwana IK, Amani H. Optimization and analysis of supply chain management performance by improving inventory management model in residential construction. International Journal of Industrial Engineering & Production Research. 2024;35(1):1–19.

[27] Imannezhad R, Avakh Darestani S. Project scheduling problem with resource constraints and activities interruption using Bees algorithm. International Journal of Industrial Engineering & Production Research. 2018;29(3):277–291.

[28] Salmasnia A, Heydarnezhad E, Mokhtari H. A robust optimization approach for a discrete time-cost-environment trade-off project scheduling problem under uncertainty. International Journal of Industrial Engineering & Production Research. 2024;35(2):1–18.

[29] Mei Z, et al. An integrated optimization and visualization approach for construction site layout planning considering primary and reuse building materials. Advanced Engineering Informatics. 2025;65:103314.

[30] Büyüközkan G, Feyzioğlu O, Ersoy MŞ. Evaluation of 4PL operating models: A decision making approach based on 2-additive Choquet integral. International Journal of Production Economics. 2009;121(1):112–120.

[31] Huang M, et al. Fourth party logistics routing problem with fuzzy duration time. International Journal of Production Economics. 2013;145(1):107–116.

[32] Yin M, et al. Fourth-party logistics network design under uncertainty environment. Computers & Industrial Engineering. 2022;167:108002.

[33] Ben-Daya M, Hassini E, Bahroun Z. Internet of Things and supply chain management: A literature review. International Journal of Production Research. 2019;57(15–16):4719–4742.

[34] Lahmine S, Bennouna F. Transforming quality management with Industry 4.0 technologies: A meta-analytic review of AI, blockchain, IoT, and big data. International Journal of Industrial Engineering & Production Research. 2025;36(2):68–79.

[35] Yu L, Shenle P. Federated digital twins platform for smart city logistics: A knowledge-driven approach. International Journal of Production Economics. 2025;109772.
[36] Le TV, Fan R. Digital twins for logistics and supply chain systems: Literature review, conceptual framework, research potential, and practical challenges. Computers & Industrial Engineering. 2024;187:109768.